NAVAL POSTGRADUATE SCHOOL
Monterey, California

THESIS

ANALYSIS OF THE SENSITIVITY OF MULTI-STAGE AXIAL COMPRESSORS TO FOULING AT VARIOUS STAGES

by

Jonathan D. Baker

September 2002

Thesis Advisor: Knox T. Millsaps, Jr.

Approved for public release; distribution is unlimited

THIS PAGE INTENTIONALLY LEFT BLANK

REPORT DOCUMENTATION PAGE			Form Approved OMB No. 0704-0188
Public reporting burden for this collection of information is estimated to average 1 hour per response, including the time for reviewing instruction, searching existing data sources, gathering and maintaining the data needed, and completing and reviewing the collection of information. Send comments regarding this burden estimate or any other aspect of this collection of information, including suggestions for reducing this burden, to Washington headquarters Services, Directorate for Information Operations and Reports, 1215 Jefferson Davis Highway, Suite 1204, Arlington, VA 22202-4302, and to the Office of Management and Budget, Paperwork Reduction Project (0704-0188) Washington DC 20503.			
1. AGENCY USE ONLY ***(Leave blank)***	**2. REPORT DATE** Sept, 2002	**3. REPORT TYPE AND DATES COVERED** Master's Thesis	
4. TITLE AND SUBTITLE: Analysis of the Sensitivity of Multi-Stage axial Compressors to Fouling at Various Stages			**5. FUNDING NUMBERS**
6. AUTHOR(S) Jonathan D. Baker			
7. PERFORMING ORGANIZATION NAME(S) AND ADDRESS(ES) Naval Postgraduate School Monterey, CA 93943-5000			**8. PERFORMING ORGANIZATION REPORT NUMBER**
9. SPONSORING /MONITORING AGENCY NAME(S) AND ADDRESS(ES) N/A			**10. SPONSORING/MONITORING AGENCY REPORT NUMBER**
11. SUPPLEMENTARY NOTES The views expressed in this thesis are those of the author and do not reflect the official policy or position of the Department of Defense or the U.S. Government.			
12a. DISTRIBUTION / AVAILABILITY STATEMENT Approved for public release; distribution is unlimited			**12b. DISTRIBUTION CODE** A

13. ABSTRACT ***(maximum 200 words)***

This thesis presents a simple, meanline analysis of the impact of blade roughness on the mass flow, work coefficient, and efficiency of a three-stage axial compressor as a function of the location of fouling. First, an extensive review is presented on the state-of-the-art of measuring compressor degradation and on the impact of roughness on loss and deviation in a compressor cascade. The performance of a baseline, three-stage compressor, which has hydrodynamically smooth blades, is predicted. Using this baseline geometry, the influence of roughness in the front, middle and rear stages is calculated using empirical data for the enhanced losses and increased deviation, with a stage stacking technique. Influence coefficients that relate percentage changes in one parameter to percentage changes in other parameters are calculated. This analysis predicts that the most sensitive parameter for predicting fouling in the front stages is the percentage change in mass flow and the most sensitive parameter for predicting fouling in the rear stages is the efficiency.

14. SUBJECT TERMS Gas Turbine, Compressor, Roughness, Fouling, Detection, Localization, Condition-Based-Maintenance			**15. NUMBER OF PAGES** 77
			16. PRICE CODE
17. SECURITY CLASSIFICATION OF REPORT Unclassified	**18. SECURITY CLASSIFICATION OF THIS PAGE** Unclassified	**19. SECURITY CLASSIFICATION OF ABSTRACT** Unclassified	**20. LIMITATION OF ABSTRACT** UL

NSN 7540-01-280-5500 Standard Form 298 (Rev. 2-89)
Prescribed by ANSI Std. 239-18

THIS PAGE INTENTIONALLY LEFT BLANK

Approved for public release; distribution is unlimited

ANALYSIS OF THE SENSITIVITY OF MULTI-STAGE AXIAL COMPRESSORS TO FOULING AT VARIOUS STAGES

Jonathan D. Baker
Lieutenant, United States Coast Guard
B.S.N.A.M.E., United States Coast Guard Academy, 1996

Submitted in partial fulfillment of the
requirements for the degree of

MASTER OF SCIENCE IN MECHANICAL ENGINEERING

from the

NAVAL POSTGRADUATE SCHOOL
September 2002

Author:

Jonathan D. Baker

Approved by:

Knox T. Millsaps, Jr.
Thesis Advisor

Young W. Kwon, Chairman
Department of Mechanical Engineering

THIS PAGE INTENTIONALLY LEFT BLANK

ABSTRACT

This thesis presents a simple, meanline analysis of the impact of blade roughness on the mass flow, work coefficient, and efficiency of a three-stage axial compressor as a function of the location of fouling. First, an extensive review is presented on the state-of-the-art of measuring compressor degradation and on the impact of roughness on loss and deviation in a compressor cascade. The performance of a baseline, three-stage compressor, which has hydrodynamically smooth blades, is predicted. Using this baseline geometry, the influence of roughness in the front, middle and rear stages is calculated using empirical data for the enhanced losses and increased deviation, with a stage stacking technique. Influence coefficients that relate percentage changes in one parameter to percentage changes in other parameters are calculated. This analysis predicts that the most sensitive parameter for predicting fouling in the front stages is the percentage change in mass flow and the most sensitive parameter for predicting fouling in the rear stages is the efficiency.

THIS PAGE INTENTIONALLY LEFT BLANK

TABLE OF CONTENTS

LIST OF FIGURES

THIS PAGE INTENTIONALLY LEFT BLANK

LIST OF TABLES

THIS PAGE INTENTIONALLY LEFT BLANK

NOMENCLATURE

ABBREVIATIONS

Roman Symbology	Definition	Units
A	Cross sectional area	m^2
B	Roughness function (Nikuradse)	
C	Chord length	m
$\vec{C}$	Absolute velocity	m/s
C_D	Discharge coefficient	[1]
ΔC_θ	Absolute change in swirl	m/s
C_f	Friction coefficient	[1]
C_p	Specific heat at constant pressure	kJ/kg-K
C_v	Specific heat at constant volume	kJ/kg-K
Δh_o	Change in stagnation enthalpy	kJ/kg
i	Incidence	Degrees
I	Fouling influence coefficient	[1]
k	Mean height of roughness elements	m
k_1	Decrease in flow coefficient	[1]
k_2	Decrease in stage efficiency	[1]
k_s	Equivalent sand roughness	m
M	Mach number	[1]
m	Deviation constant	
$\dot{m}_a$	Air mass flow	kg/s
N	Rotational speed	RPM
n	Stage number	
P	Static pressure	Pa
P_T	Stagnation pressure	Pa
ΔP_{intake}	Intake depression	Pa
R	Gas constant for air	J/kg-K
Re	Reynolds number	

$\overline{R}_z$	Relative roughness	[1]
$S = \frac{C}{s}$	Solidity	[1]
s	Spacing	m
T	Static temperature	K
T_T	Stagnation temperature	K
U	Free stream velocity	m/s
U	Wheel speed	m/s
$\vec{W}$	Relative velocity	m/s
w	Work	kJ/kg
ΔW_θ	Relative change in swirl	m/s
Y	Throttle expansion factor	

Roman Symbology	**Definition**	**Units**
α	Absolute angle	Degrees
β	Relative angle	Degrees
δ	Deviation	Degrees
δ_2	Momentum boundary layer thickness	m
η	Adiabatic Efficiency	[1]
$\phi = \frac{Cz}{U}$	Flow coefficient	[1]
γ	Airfoil camber angle	Degrees
$\gamma = \frac{C_p}{C_v}$	Ratio of specific heats	[1]
λ	Stagger angle	Degrees
ν	Kinematic viscosity	m^2/s
$\varpi = \frac{P_{T1} - P_{T2}}{P_{T1} - P_1}$	Total Pressure Loss Coefficient	[1]
$\pi = \frac{P_{T2}}{P_{T1}}$	Total Pressure Ratio	[1]
ρ	Density	kg/m^3

$\psi = \frac{\Delta C_\theta}{U} = \frac{\Delta h}{U^2}$	Pressure (or work) coefficient	[1]
τ_w	Skin friction or shearing stress	Pa
$\tau = \frac{T_{T2}}{T_{T1}}$	Total temperature ratio	[1]

NOTATION

CBM	Condition Based Maintenance
EGT	Exhaust gas temperature
IGV	Inlet guide vane
ISO	International standard organization
NACA	National Advisory Committee for Aeronautics
PMS	Preventative Maintenance Schedule

SUBSCRIPTS

abs	Absolute
b	Boyce (deviation)
c	Carter (deviation)
c	Compressor
corr	Corrected
f	Fouled
h	Hub
k	Roughness elements
r	Rotor
rel	Relative
s	Shakhov (deviation)
s	Stator
st	Stage
t	Tip
z	Axial

THIS PAGE INTENTIONALLY LEFT BLANK

I. INTRODUCTION

A. MOTIVATION

The United States Navy and Coast Guard are shifting their approach to machinery maintenance. Preventative Maintenance Schedules (PMS) once prescribed maintenance based exclusively on hours of operation or a scheduled time interval since the last servicing. PMS guidelines were developed with field experience and conservatism in mind, thus providing adequate maintenance schedules to maintain machinery in peak operational condition. However, the major drawback of such a rigid system is the tendency to conduct overhaul or preservation procedures on components that don't actually require repair. As stated in OPNAV 4790.16 [53], unnecessary maintenance contributes to inflated ownership costs and reduced readiness for deployable assets.

Recently, the U.S. Navy instituted a Condition Based Maintenance (CBM) system to operate in conjunction with a modified PMS program. By monitoring and recording trends in system performance characteristics (e.g. increase in vibration) and comparing to published threshold values, CBM eliminates many nonessential repair procedures that would have previously been performed without question. Proper application of CBM practices, as part of an overall maintenance effort, can reduce operating and support (O&S) costs and manpower requirements by providing a basis for maintenance decisions that focuses limited resources on maintenance most needed to ensure safety and mission readiness [53].

One area of interest in CBM is gas turbine compressor cleaning (washing) to remove fouling. Compressor fouling is the buildup of particulate deposits on the rotating (rotor) and stationary (stator) airfoils. Of the numerous contributors to gas turbine performance degradation, compressor fouling has the greatest impact [10]. Gas turbine performance deterioration due to compressor fouling is mainly recoverable through washing.

Compressor fouling makes a gas turbine hard to start, reduces peak power, fuel efficiency, and the stall margin, and may damage the engine. The problem is that even a badly fouled compressor operating at a low power level may not exhibit telltale signs of

fouling. Therefore, a parameter used as an indicator of fouling should be as sensitive as possible to fouling. Operators need a simple and reliable method for detecting fouling at a level where performance can be restored by compressor cleaning [10, 68].

The Rolls Royce/Allison 501-K17 and K34 are used for electric power generation on most U.S. Navy surface combatants. Crank washing of the compressor to remove fouling deposits is performed by rotating an off-line gas turbine at low speed while spraying a detergent solution into the bellmouth, followed by a water spray. The crank washing procedure requires operators to: 1) Secure (Tag-Out) several gas turbine subsystems, 2) Prepare the wash tanks with the appropriate solutions and pressurize with ship's service air, 3) Perform the crank wash, 4) Clean up and dispose of the residual wash chemicals (typically a hazardous material), 5) Line up and activate the previously secured subsystems (Tag-In), 6) Start and run the turbine for several minutes to dry the interior surfaces and components, and 7) Check turbine parameters to see if performance was recovered. The crank washing process is expensive, time consuming, results in generator down time, and subjects the turbine to additional wear and tear. Washing the compressor only when cleaning is required is therefore quite preferable to cleaning at a set number of operational hours or time interval.

B. BACKGROUND

The 501-K34 uses about $3.5 \cdot 10^6$ lbm of air per day when in operation. With this massive rate of air ingestion, even if the contamination level of the air after the filters is only 3 ppm, the gas turbine ingests over 10 pounds of foreign material per day. This example illustrates why the ingestion of airborne particles is such an important factor causing performance deterioration in all types of gas turbines.

Aerodynamically, an axial compressor is very sensitive to changes in airfoil shape and roughness, requiring close tolerances on blading for baseline performance to be achieved. Performance degradation is generally due to 1) Fouling deposited on blade surfaces, 2) Erosion and an increase in tip clearance due to abrasion of ingested contaminants, and 3) Water ingestion from rain or saltwater spray. Of these main contributors to performance reduction, axial compressor fouling is the most significant problem faced by operators in marine applications. Compressor fouling is typically responsible for about 75% of all gas turbine performance loss [10, 19].

1. The Nature of Compressor Fouling

Fouling is due to the adherence of particles to airfoil & annulus surfaces, which increases surface roughness and changes the geometric shape of components in the air stream. Hard contaminants (e.g. dust, ash, dirt, sand, rust) less than 10μm in diameter generally cause fouling and those larger than 10μm can also cause erosion [37, 46, 78]. Soft particles such as airborne salts, oil and unburned hydrocarbons cause fouling only.

Fouling deposits on the blade pressure side are caught by impact, but studies have shown that foulants also adhere to the suction side [10, 46]. The leading edge has the highest deposition rate [7], being about an order of magnitude greater than the rest of the blade surface, for both rotor and stator. The mechanism governing leading edge and rotor pressure surface fouling is inertial impaction [7]. Diffusion dominates particle deposition on the rotor suction side and both stator surfaces [7], thus deposits are typically smaller and lighter. Rotor suction side fouling is similar to dust accumulation on the low-pressure surfaces of a household fan.

Deposits are a mixture of water-wettable, water-soluble and water insoluble materials, often of PH=4 or lower, increasing the risk of pitting corrosion [78]. Water-soluble compounds cause corrosion since they're hygroscopic (moisture absorbing) and/or contain chlorides that promote corrosion. They can be rinsed, but many are also imbedded in water-insoluble compounds. Water insoluble compounds are mostly organic such as hydrocarbon residues. Left untreated, fouling deposits become more difficult to remove as the aging process bonds them more firmly to airfoil surfaces. Humidity normally exists in the form of liquid droplets and vapor through about the first half of the compressor stages, increasing the "sticking" probability for deposits and salt particles [77]. Additionally, higher relative humidity exists at the inlet due to the static pressure drop during airflow acceleration across the bellmouth (nozzle), favoring the precipitation of contaminants on the blades. As the air progresses through the compressor it becomes hotter and drier, generally causing less fouling in the latter stages [91].

Compressor deterioration (due to fouling) is exacerbated by internal oil leaks near the blade surfaces. Oily substances in the incoming air act as glue to fix dirt particles to

compressor airfoil and shroud surfaces. In the high temperature region at the back end, oils bake onto surfaces and forms a thick coating.

Fouling rates vary significantly due to compressor aerodynamic design, site location and surrounding environment and climate. Weather has proven to have the greatest impact on fouling rate [78, 91].

2. Sensitivity and Susceptibility to Fouling

The inherent sensitivity of an axial compressor to fouling is determined by the air inlet velocity at the inlet guide vanes, compressor pressure ratio, aerodynamic and geometric characteristics. Researchers have debated whether small gas turbines (less than 3 MW) have a greater sensitivity to fouling [82] than large engines [64]. The consensus has been that the stage loading has the main influence [61, 67, 68]. Whether the gas turbine is large or small, fouling will be more detrimental to a compressor with heavily loaded stages (positive incidence) than one with lightly loaded stages (zero or negative incidence). Hence, fouling is most deleterious to the performance of a gas turbine operating at peak load conditions.

It has been established that smooth airfoil surfaces, or those with coatings, are less susceptible to fouling and respond better to cleaning by washing [14, 42]. Fouling rates typically decrease as the ambient temperature decreases [31, 37]. Humidity increases the fouling rate up to a certain point: Above a certain humidity level, the condensed water droplets in the air flow will wash the blading (naturally), and power losses due to fouling may be reduced [19, 60, 78].

C. OBJECTIVES

The objectives of this study were to determine, based on a first order physical model of the flow at mid span of a three-stage axial compressor:

1. The most sensitive and reliable parameter to indicate that fouling is present.
2. The best parameter or group of parameters to localize in which stage(s) fouling exists.

D. ORGANIZATION

Chapter II presents an extensive review on the state-of-the-art on measuring compressor performance degradation due to fouling, localization and the impact of roughness on loss and deviation in a compressor cascade.

Chapter III describes the development of a simple, meanline analysis of a three-stage compressor model, which has hydrodynamically smooth blades. Using this baseline geometry, the influence of roughness in the front, middle and rear stages is separately calculated using empirical data for the enhanced losses and increased deviation, with a stage stacking technique.

Chapter IV contains the results of the fouling simulation. An influence coefficient that relates the percent change in mass flow to the percent change in efficiency is calculated.

Chapter V presents a summary of the findings of this study and provides conclusions based on those findings. Recommendations for future work are given.

THIS PAGE INTENTIONALLY LEFT BLANK

II. STATE OF THE ART IN COMPRESSOR FOULING, DETECTION, AND LOCALIZATION

A. GENERAL DISCUSSION

The reduction in gas turbine performance due to compressor fouling is gradual, but increases rapidly (some authors say "exponentially") if the compressor isn't washed in time [10, 46, 78]. Three types of performance deterioration are typically described:

1. *Recoverable* with cleaning/washing, such as deposits on the blades which may be washed off;
2. *Non-recoverable* with cleaning/washing, such as baked-on contaminants that must be physically scraped off the airfoils (during an overhaul); and
3. *Permanent* deterioration such as blade leading edge and tip erosion, which is not recoverable by overhaul (unless blades are renewed).

Performance deterioration due to fouling is mostly recoverable [8, 10, 37].

B. ROUGHNESS

1. Definition of Roughness

Fluid moving across a surface is subjected to resistance if the surface is rough. The resistance due to roughness depends on the density distribution of the roughness elements (number per unit area), the shape and height of the roughness elements, and their geometrical arrangement over the surface [17].

The shape and density distribution of the protrusions will vary significantly from one practical application to another. Therefore, it is convenient to correlate a given mean roughness height, k, with a standard roughness. It is common to adopt Nikuradse's [17] equivalent sand roughness, k_s. Roughness element height, k, is converted to equivalent sand roughness, k_s, by the equation:

$$5.75\log\left(k_s \diagup k\right) = 8.5 - B \tag{1}$$

where B is a dimensionless roughness function based on the Reynolds number of the roughness elements. For a hydrodynamically rough surface, $B = 8.5$, so $k = k_s$. For a hydrodynamically smooth surface, B is typically less than 8.5, so $k_s > k$.

2. The Effect of Surface Roughness of a Cascade

a. Hydrodynamically Smooth Versus Rough

Roughness will degrade performance if a blade is hydrodynamically rough. The Reynolds number of the roughness elements is calculated to estimate if a compressor blade is rough, using

$$\mathrm{Re}_k = \mathrm{U}k/\nu \tag{2}$$

where U is the free stream velocity, k is the roughness element height, and ν is the kinematic viscosity of air. If this Reynolds number is less than 100, the roughness peaks are contained within the viscous sublayer and the blade is hydrodynamically smooth. Schlichting [71] gave the criterion for hydraulic smoothness on flat plates a value of Roughness Reynolds Number < 100, based on equivalent sand grain roughness and free stream velocity.

$$\mathrm{Re}_k < 100 \qquad [C_f = f(\mathrm{Re})] \rightarrow \text{Smooth} \tag{3}$$

$$100 < \mathrm{Re}_k < 1000 \qquad [C_f = f(\mathrm{Re}, k)] \rightarrow \text{Transitional} \tag{4}$$

$$\mathrm{Re}_k > 1000 \qquad [C_f = f(k)] \rightarrow \text{Fully Rough} \tag{5}$$

While this is strictly true for flat plates which have no pressure gradient, it also applies, at least approximately, for airfoils where $dP/dx \neq 0$. For typical parameters, such as U=200 m/s and $\nu = 1.5 \cdot 10^{-5}$ m^2/s, this means that if the blade has a surface finish of 1 μm (39 μin), it is very smooth. It is not beneficial to make airfoils any smoother than this.

b. Effect of Roughness on the Boundary Layer

The surface quality of the blading greatly affects the efficiency of energy conversion in a turbomachine [6]. Fouling causes an increase in surface roughness and changes the blade shape if a sufficiently thick layer is added. Added roughness, when the blade is hydrodynamically smooth, increases the momentum boundary layer thickness,

δ_2, and increases the risk of flow separation. When the tips of roughness elements protrude through the viscous sublayer in the turbulent regime, the skin friction, τ_w, is increased [37], and separation conditions are reached before the trailing edge of the chord [41].

Since the suction surface of an airfoil sees greater local velocities than the pressure surface, the suction side is more sensitive to roughness. The boundary layer and viscous sublayer are thinner on the suction surface, so roughness elements are more prone to create disturbances and "trip", or transition the flow to turbulance early, particularly on the adverse pressure gradient part of the blade. Rotor blades are similarly most sensitive when roughness accumulates toward the leading edge.

c. Profile Loss

The total pressure loss produced by the blades in the cascades, away from the endwall, is often called profile loss [17]. For compressible flow, profile loss is defined as

$$\varpi = \frac{P_{T2} - P_{T1}}{P_{T1} - P_1} \tag{6}$$

the increase in total pressure across an airfoil divided by the difference between the upstream total and static pressure. For smooth blades in a cascade, profile loss, ϖ, is a function of blade profile, solidity, S, Mach number, M, and incidence, i.

A small displacement of the flow separation point in the upstream direction significantly increases the losses [6]. The wake region becomes more extensive and pronounced, leading to greater total pressure losses. The main influence of blade roughness appears around optimum incidence angles, while the "far-off-optimum performance" is hardly affected, as discussed by Bammert and Woelk [6]. It is clear that added roughness on the pressure side has a very small effect compared to the suction side, as discussed by Kurz and Brun [37]. Milsch [8] found an increase in profile losses for NACA 65(12)06 compressor cascades from 2% (ϖ = 0.02) with k_s/C = $0.3 \cdot 10^{-3}$, to 10% (ϖ = 0.10) with k_s/C = $5 \cdot 10^{-3}$, where k_s is the equivalent sand roughness and C is the chord.

d. Turning

The "turning" in a cascade is analogous to lift in an isolated airfoil. Turning is limited by boundary layer separation on the suction (or perhaps pressure – negative incidence stall) surface of a rotor or stator airfoil.

One might expect roughness on an airfoil to increase the deviation angle (reduce turning) if the blade is hydrodynamically smooth ($\mathrm{Re}_k < 100$), although there is very little quantitative data available to confirm this. Mal'tsev and Shakhov [41] performed airflow turning tests on plane compressor cascades with solidities of 1.21 and 1.53, 28 degrees of camber, and wind tunnel stream velocity U = 33 m/s. This leads to a Reynolds number based on chord of 240,000, which is near the range where the total pressure loss is sensitive to Reynolds number [57]. Relative roughness ($\overline{R}_z = k/\mathrm{C}$), which is the roughness height, *k*, divided by the blade chord, C, was varied from $1.3 \cdot 10^{-3}$ to $16.7 \cdot 10^{-3}$. The levels of roughness used in the experiments were chosen to match the levels that were measured in real helicopter engine blading after 1,500 hours of service. For the test setup, relative roughness of $\overline{R}_z < 0.4 \cdot 10^{-3}$ was hydrodynamically smooth [41].

In the first set of experiments, the incidence, *i*, was varied with fixed roughness. In the second set of experiments, incidence was fixed and roughness varied. Measurements were made of: 1) Change in flow lag angle, or deviation angle, δ, with different solidity and variation of roughness, and 2) Variation of the derivative of flow turning angle with respect to the incidence as a function of roughness. The paper presented the results both in graphical form and provided an equation for a curve fit of these data:

$$\delta = K_1 + K_2(\overline{R}_z)^{1/2} + K_3(\overline{R}_z) + (K_4 + i)^2\left(\frac{1}{K_5} + \frac{1}{K_6}(\overline{R}_z)^{1/2}\right) - K_7\left(\frac{\mathrm{C}}{s} - K_8\right) \qquad (7)$$

where C is the chord, *s* is the blade spacing (C/*s* = solidity), K_1=6.9°, K_2=20.4°, K_3=17.9°, K_4=10.0°, and K_7=3.1°; K_5=519.0, K_6=27.0, and K_8=1.2 [41].

C. THE EFFECT OF FOULING ON A COMPRESSOR

Many studies have shown that the main effect of compressor fouling is a reduction of mass flow, $\dot{m}_a$, and that the percent reduction increases with operational speed [10, 21, 35, 63, 64, 65, 67, 68, 91]. Fouling also reduces the compressor pressure ratio, π_c, and adiabatic efficiency, η_c, causing a decrease in gas turbine power output and an increase in heat rate [35, 64, 91]. Fouling reduces the operating range (on the compressor map) and shifts the operating point to lower mass flow rates at a given corrected speed. Fouling also decreases the specific work, *w*, which results in a further drop in power output. Roughness makes the constant speed lines steeper on the compressor map, thus the range of mass flow rates covered by the characteristic curves decreases. The attainable pressure ratios are reduced (stall line drops) [6, 67].

For a single-shaft gas turbine experiencing typical compressor fouling in the front stages, the percent reduction in air inlet mass flow is greater than the percent change in compressor pressure ratio, which is in turn greater than the percent decrease in compressor adiabatic efficiency. For any gas turbine undergoing front stage fouling, the percent decrease in airflow is typically 2-3 times greater than the percent decrease in efficiency [8, 10, 35, 37, 64].

D. FOULING DETECTION

1. General Discussion

Condition based compressor cleaning requires close monitoring of engine parameters and development of a system that can predict performance degradation as a result of compressor fouling. An ideal parameter to monitor for an indication of fouling 1) Provides an accurate, repeatable indication of compressor condition, 2) Should be unaffected by changes in external variables (e.g. ambient conditions or process load), 3) Requires simple and quick data collection, and 4) Allows for simple interpretation of the data, regardless of the operator's knowledge of turbomachinery. These desirable characteristics were never found for any parameters or combination of parameters examined [10, 31]. However, the change in compressor pressure ratio or air intake depression provides a good assessment of compressor fouling when corrected to standard conditions.

2. A Comparison of Parameters to Detect Fouling

Compressor Temperature Rise Coefficient ($\tau_c = T_{T,out} / T_{T,in}$): This quantity is not considered a reliable parameter to identify fouling influence [4, 31, 37, 65]. Temperature rise is affected by fouling, but its value can be higher or lower when compared to "as new" condition. Tests by Aker and Saravanamuttoo [65] found that a small, moderately loaded gas turbine compressor (Solar Centaur) experienced no change in τ_c, with up to 20% of the stages fouled, then a slight increase was noted as additional stages were fouled. Experiments by the same authors [65] on a large, heavily loaded compressor (LM-2500) resulted in a drop in τ_c with the front stages fouled, then a small increase was seen as the rear stages were fouled [65]. This is because when a compressor fouls, there is a reduction in rotor turning (ΔC_θ), which results in a decrease in work done by the rotors, and reduces the compressor temperature ratio, τ_c.

Exhaust Gas Temperature (EGT): The compressor, combustor, and turbine all influence a gas turbine's exhaust gas temperature. Compressor fouling, turbine fouling, erosion or leaks, and fuel nozzle deterioration may result in an increase in EGT for a given power output. Therefore, EGT is a poor parameter to indicate compressor fouling.

Compressor Efficiency (η_c): Compressor efficiency is not considered sensitive or accurate enough to consistently determine the degree of fouling [31, 37, 65]. The temperature and pressure at the back end of the compressor are subject to a high degree of scatter and must be averaged. Hence, comparison with a reference point is difficult and not precise [91]. Compressor efficiency has also been shown to lack the power to be an accurate indicator of fouling location [91].

Site Horsepower: There are too many variables associated with accurately measuring the gas turbine power output. Compressor mass flow and the total inlet and outlet temperatures are all required. Also, the Allison 501-K generates power to match the needs of the ship. Hence it may not be measured directly and is a poor parameter to indicate fouling.

Compressor Pressure Ratio ($\pi_c = P_{T,out} / P_{T,in}$): This is one of the more effective methods of measuring compressor deterioration. The pressure ratio always decreases

with increased fouling. However, the airflow at the compressor outlet is hot and non-uniform, making an accurate measurement of total pressure difficult.

Air Intake Depression (ΔP_{intake}). Intake depression is the static pressure drop across the bellmouth, or the difference between the total and static pressure at the throat (assuming P_T is constant across the bellmouth). Originally proposed by Scott in 1979 [73], intake depression is simple to measure, inexpensive and relatively non-intrusive. If there is room for an additional pressure tap to install at the compressor inlet, this may be the most accurate and sensitive of all parameters for the assessment of fouling [10, 19, 31, 73].

Only three measurements are required to measure the inlet mass flow: The total temperature (T_T), total pressure (P_T) and static pressure (P) at the bellmouth throat. Thus, monitoring ΔP_{intake} is a method to accurately ascertain the corrected mass flow. Intake depression is simpler to measure than π_c or η_c. The corrected mass flow, $\dot{m}_{a,corr}$, can be compared with the corrected speed, N_{corr}, as an indicator of fouling.

The decrease of compressor intake depression from "clean engine" conditions has proven to be an excellent indicator of fouling. When a compressor fouls, the decrease in mass flow rate is roughly proportional to the square root of the change of intake depression [73]. Hence, intake depression is significantly sensitive to changes in mass flow rate.

Remote oil pumping stations in the Saudi Arabian desert, where ambient conditions generally exceeded 110˚F and dense, airborne dust was almost always present, have successfully employed intake depression monitoring to use as a decision tool to determine when to wash [31]. In other pipeline applications where fuel economy is always critical, compressors were washed when a 3% reduction in intake depression was detected [67]. This is about a 1.3% reduction in the baseline, clean mass flow. Cleaning at this stage of degradation restored intake depression (and mass flow) to the original level.

Once the level of deterioration is known, cost-benefit analysis can be performed to determine the most economical time to clean. Though some operators may disagree,

gas turbine efficiency is likely the most important on-condition basis parameter [10], as it limits the amount of operating time in an uneconomical condition. Such is the case for remote pumping stations where fuel supplies are limited. If maximum power is always desired, even a small amount of fouling can pose significant problems, as the power reduction due to fouling is the greatest for a peak load unit. In such a case there is little to be gained from on-condition compressor cleaning; Frequent, regularly scheduled washing should be the standard [10, 65].

E. LOCALIZATION OF FOULING

In 1980, Zaba's [91] simulation studies with a 16-stage compressor showed that the reduction in efficiency and mass flow due to fouling is highly dependent on location (i.e. front stages fouled, rear stages fouled. or uniform fouling throughout). He introduced a fouling influence coefficient, $I_{\dot{m}_a,\eta_c}$, to separate losses caused by deposits according to their location in the compressor (or turbine for that matter). We'll assume negligible turbine fouling. Zaba's fouling influence coefficient was:

$$I_{\dot{m}_a,\eta_c} = \frac{\partial \dot{m}_a / \dot{m}_a}{\partial \eta_c / \eta_c} = \frac{\partial \dot{m}_a}{\partial \eta_c}\frac{\eta_c}{\dot{m}_a} \tag{8}$$

where compressor efficiency is

$$\eta_c = \frac{\pi_c^{\frac{\gamma-1}{\gamma}} - 1}{\tau_c - 1} \tag{9}$$

temperature rise coefficient is $\tau_c = \frac{T_{T,out}}{T_{T,in}}$, and pressure ratio is $\pi_c = \frac{P_{T,out}}{P_{T,in}}$.

The possible scenarios include:

If $I_{\dot{m}_a,\eta_c} \cong 1$ ($\%\Delta\dot{m}_a \cong \%\Delta\eta_c$), this is an indication that there is uniform roughness (fouling) of the compressor from front to rear, which is uncommon. Zaba's simulation results confirm that $I_{\dot{m}_a,\eta_c} = 1$ for uniform fouling within 0.053% [91]. Bammert's work [6] on blading surface roughness the previous year confirmed this idea, though he didn't comment on it.

If $I_{\dot{m}_a,\eta_C} > 1$ ($\%\Delta\dot{m}_a > \%\Delta\eta_c$), this is an indication that the front stages are more heavily fouled, which is typical. Zaba found that fouling of the early stages had a greater influence on the mass flow rate than the latter stages. Stage loading (ψ_{st}) peaks in the first few stages, corresponding to reduced stage flow coefficients (ϕ_{st}). The "cumulative effect" progresses through the compressor, as all the remaining stages are forced to operate at reduced flow coefficients, resulting in a marked decrease in air mass flow. Boundary layer growth results in a reduction in flow area, reducing the mass flow as well. Hence, the percent reduction in mass flow is greater than the percent reduction in efficiency.

For the most part, the change in efficiency due to added roughness on a particular stage, η_{st}, is a very weak function of the stages upstream and downstream of it. Therefore, Zaba's [91] compressor efficiencies were nearly the same (within 0.7%) for cases of fouling in the early and later stages. This is why the ratio of percentage change in mass flow, which is sensitive to location, divided by the percentage change in compressor efficiency, which is a weak function of location, is an indicator of fouling location.

If $I_{\dot{m}_a,\eta_C} < 1$ ($\%\Delta\eta_c > \%\Delta\dot{m}_a$), this is an indication that the rear stages are more heavily fouled, which is uncommon, but may occur due to oily deposits that are baked on over time. Rear stage fouling causes heavier aerodynamic loading in the middle stages and can result in flow separation in these stages. The fouled latter stages are aerodynamically unloaded. Stage loading (ψ_{st}) peaks in the middle stages, resulting in a smaller "cumulative effect" progressing through the compressor than for the case of early stage fouling. As a result, the percent reduction in mass flow is not as great for rear stage fouling. Again, compressor efficiency is about the same for front and rear stage fouling (deposits of the same magnitude), so the percent reduction in efficiency is greater than the percent reduction in mass flow.

Other influence coefficients, which indicate ratios of percentage changes in two parameters, may be calculated to see if they provide information on fouling location. Examples include, but are not limited to:

$$I_{\dot{m}_a,\pi_c} = \frac{\%\Delta\dot{m}_a}{\%\Delta\pi_c},\ I_{\dot{m}_a,\tau_c} = \frac{\%\Delta\dot{m}_a}{\%\Delta\tau_c},\ I_{\eta_c,\pi_c} = \frac{\%\Delta\eta_c}{\%\Delta\pi_c}, \text{ and } I_{\pi_c,\tau_c} = \frac{\%\Delta\pi_c}{\%\Delta\tau_c}$$

F. FOULING SIMULATION

1. General Discussion

A systematic investigation of compressor fouling requires that the effect of fouling of a single stage be modeled correctly and hence the overall effect on compressor performance can be obtained from the effects of the fouling on the constituent stages [10]. In compressor performance deterioration studies, the variation in the compressor map due to fouling is sought [10, 68]. Simulation exercises can provide a quantitative estimate of how severely engine performance will suffer from fouling of various magnitudes and at different locations. The information can then be used to evaluate the most economical interval between compressor washes, or to determine an appropriate fouling threshold (limit) if on-condition washing is desired [10, 65, 77, 80].

2. Stage Stacking Technique

a. Stage Stacking Development

Stage stacking was developed in 1957 by Stone [80] to aide in compressor design, mainly for prediction of stall and surge limits. He calculated stage pressure and temperature ratios for each compressor stage. Stage flow coefficients were then calculated from continuity. An area schedule was assumed that reduced through the compressor corresponding to the pressure rise to yield constant axial velocity at the design point throughout [80].

For a simple, qualitative comparison, Stone neglected Mach number effects and assumed incompressible flow. When the first stage operates at an elevated density ratio due to working at a higher pressure (work) coefficient and/or speed than design (fouling), the second stage operates at a lower flow coefficient, and hence a higher work coefficient than stage one. The second stage density ratio is even higher above design than stage one. This effect is cumulative through the compressor until the flow coefficients become sufficiently low to cause stage stall, whence the rate of flow coefficient reduction diminishes. The converse is true when the first stage operates

below its design density ratio. Hence, Stone was able to establish stall and choking limits.

b. The Modern Application of Stage Stacking

Stage stacking is used predominantly to predict the behavior and performance of gas turbines during off-design operation [76]. On-site measurable values compared with baseline (clean engine) conditions are utilized.

Compressor performance is normally depicted by its stage characteristics, which are the stage flow coefficients, $\phi_{st} = {c_z}/{U}$, pressure (or work) coefficients, $\psi_{st} = {\Delta C_\theta}/{U} = {\Delta h_o}/{U^2}$, temperature ratios, $\tau_{st} = \frac{T_{T,out}}{T_{T,in}}$, and efficiencies, η_{st}, from Equation (9). These stage performance characteristics describe the variation of compressor pressure ratio and efficiency with engine mass flow rate [10, 58]. Stage stacking takes into account interrelationships among stages through compatibility of speed, mass flow and energy. Thus it provides a logical basis for examining the behavior of a multistage compressor subjected to deterioration (i.e. fouling) in one or more stages. The performance of a multistage axial compressor is determined with a stage-by-stage sequential calculation. Calculation is straightforward for a fixed geometry compressor, such as the Allison 501-K.

Compressor performance can be accurately predicted at design conditions. Off design conditions are still a problem. If suitable stage performance representations can be acquired or estimated, engine performance over a range of operating conditions can be predicted with reasonable accuracy. For example, the influence of different types and locations of compressor fouling on overall compressor performance can be investigated by appropriately modifying the compressor map [64]. Given a particular rotational speed and airflow rate, the axial velocity, static pressure and temperature at the first stage inlet are obtained with the continuity equation. The flow coefficient is obtained from the axial velocity and rotational speed, while total pressure and temperature at the first stage outlet are determined using the performance curves. Axial velocity (C_z), static pressure (P_2) and temperature (T_2) at the first stage outlet are determined using the continuity equation and are used as the inlet conditions for the

second stage. The calculation process proceeds sequentially to the last stage in order to obtain the values for compressor exit temperature and pressure.

Compressor performance specifications are typically proprietary in nature. So, when stage characteristics from test data are not available they may be estimated fairly accurately with stage geometry, blade rows and flow patterns [68]. The sequential calculation process requires an accurate measurement of the air mass flow rate, not just the state variables at inlet and outlet. Stage stacking becomes cumbersome and subject to error if iteration is necessary to obtain a mass flow rate that satisfies the boundary conditions at each end of the compressor [76]. This is another reason why intake depression is quite desirable, as it yields an accurate assessment of mass flow.

c. A Successful Field Application

Before the operator can make an informed decision to wash the compressor, it is necessary that he be able to predict the performance of the gas turbine over its expected running range. In 1983, Saravanamutto and MacIssac [69] conducted a very simple fouling simulation analysis on pipeline gas turbines (Rolls Royce Avon, ~3 MW). Fouling thresholds were needed for in-service monitoring to save on fuel and repair costs. Thermodynamic models capable of predicting the entire operating range expected were required. From compressor meanline data the authors simulated significant fouling with a 7% reduction in mass flow and a 2% reduction in efficiency and implemented this on the compressor characteristics by multiplying all stage flow rates by 0.93 and efficiencies by 0.98. The compressor was found to still operate within stall and surge margins over the range of typical operating conditions. Intake depression measurement equipment was installed to monitor inlet air mass flow and a conservative 5% reduction threshold (for washing) was applied. This cleaning program was successful at consistently restoring compressor performance.

3. Linear Progression of Fouling

Aker and Saravanamuttoo [65] have investigated the validity of a linear progression of fouling in compressor stages on GE LM2500 and Solar Centaur oil pipeline gas turbines. A stepwise calculation is used to model the buildup of contaminants in the compressor by modifying the appropriate stage flow and efficiency characteristics. As described previously, it is accepted that the impact of fouling on the

front stages of the compressor is greater than on the rear stages. To model this, the authors reduced the stage flow coefficients by a certain percentage (k_1%) through a linear progression from (n x k_1) for the first stage through k_1 for the nth stage. Stage efficiency was similarly decreased by a factor of (k_2%). This particular model of fouling is called "k_1: k_2".

This linear fouling model assumes fouling progresses in steps, where each step increases the number of stages affected by one and the level of flow reduction by 1%. For the first step a 1% reduction in flow coefficient for the first stage (ϕ_1) is made. For the next step, a 2% reduction in the flow coefficient for the first stage and a 1% reduction for stage two (ϕ_2) is made, and so on. It has been seen that the drop in efficiency for front stage fouling is a function of the percentage of flow coefficient reduction. A 0.25% reduction in stage efficiency (η_{st}) was applied for each step (corresponding to each 1% reduction in stage flow coefficient). Hence, the model was (1:0.25). This linear progressive fouling model was found to work well up to the middle stages [63].

G. THE EFFECT OF BLEED AIR

No fouling experiments were found in the literature that considered compressor bleed air. However, there are a few experiments that have examined the effect of interstage bleed air on the overall compressor map, specifically on inlet airflow. As shown by Sten'kin [79], the effect of compressor bleed on inlet air flow seems to be related to the slope of the pressure head line of the upstream stages and the magnitude of the bleed. As such, Sten'kin proposed that the increase in $\dot{m}_a$ due to bleed:

$$\left(\left| K \right| \Big/ (1-K) \right)^{X} \times \left(\dot{m}_{a,bleed} \right) \tag{10}$$

where

$$K = \left(\partial \ln \dot{m}_a \Big/ \partial \ln \pi_c \right) \tag{11}$$

The X is an approximate exponent specific to a compressor. Sten'kin's 7-stage axial compressor had X = 0.35, which was empirically fit.

In a study where bleed devices were placed at several stage locations in a compressor cascade, bleeding always increased the inlet air mass flow [76]. That is to

say, $\dot{m}_{a,inlet,initial} < \left(\dot{m}_{a,outlet,w/bleed} + \dot{m}_{bleed}\right)$. Simulation studies have shown that compressor performance is highly dependent on the location of bleeding [76]. An extraction at earlier stages leads to higher delivery mass flow rates than extraction at later stages. Bleed seems to have little impact on compressor efficiency and pressure ratio. The influence is mainly on compressor mass flow.

H. CLEANING METHODS

1. General Discussion

The injection of solid compounds (rice husks or nutshells – soft erosion on-line cleaning) has been replaced by wet cleaning since the introduction of coated compressor blades for pitting prevention [45]. The three types of cleaning are hand cleaning (which is actually quite effective for IGVs and first stage rotor fouling, which have the greatest impact on performance degradation), on-line (at part-load operation), and off-line crank washing.

2. Off-Line Crank Washing

The turbine is motored at very slow speed (less than 15%, ideally) while injecting detergent at the inlet, followed by a soaking period, then concluded with a demineralized water rinse. Crank washing can be more effective than on-line washing, but is more time intensive and disruptive to operations. The main constituent of the cleaner is its surfactant (surface-acting-agent), which reduces the surface tension of the solution, enabling it to wet, penetrate and disperse deposits. Water films drain off blades rapidly, reducing the contact time during the off-line soaking period. Foam, however, is an excellent dirt carrier. The amount of foam generated by a compressor cleaner is an indication of the degree of activity and therefore the effectiveness of the surfactants.

Crank washing with cleaning solvents at relatively cold temperatures (~15°C) has proven to be most effective [1, 78]. However, experiments have also shown that crank washing with hot, distilled water can be nearly as effective at removing oily deposits as solvent cleaning [47]. The water is heated to near the boiling point by compressor bleed air. Compressor air is also used to displace the water out of its reservoir for cleaning.

3. On-Line Washing

Demineralized water and/or cleaning solution are injected at the inlet under part-load operation. This is less disruptive and time intensive than off-line crank washing. Little or no cleanup is required. On-line washing is not as effective as crank washing due to increased rotational speed – centrifugal forces spread the solution to the casing surface after only a couple of stages. The overall effect is more like a "steam cleaning" [33, 36, 78].

The rate of fouling is slowed by frequent on-line water washing. More significant performance recovery is obtained through off-line crank washing. No matter how good the wash, the rear stages of the compressor will not get cleaned; Hand cleaning or overhaul is necessary in such a case [33].

4. Optimum Regimen

Frequent on-line cleaning increases the allowable time interval between off-line cleaning operations. On-line washing with water should be conducted at short intervals (every 3 days to weekly). On-line cleaning with detergent cleaners should be conducted once a week at most. A general recommendation for crank washing is to clean/wash when the estimated inlet air flow decreases 2-3% [40, 73]. Furthermore, at least four off-line cleanings per year are needed to remove salt-laden deposits on the downstream stages. This rule also holds for a peak load unit running only a few times a week [1, 19, 36, 45].

Some authors recommend an on-line wash every 200 hours and soak/crank-wash every 1000 hours [67]. Others suggest a maximum interval between on-line washes of five days, thereby assuring little ageing of the deposition layer [47]. In general, operators should perform an on-line wash frequently to remove salt deposits, regardless of performance. If the on-line wash is not effective at restoring performance, a crank wash should be performed. The cleaning liquid should be viscous enough to cling to the blades during the spraying and soaking period, then be easily dissolved and removed thereafter during rinse. Engine cranking at very slow speed is preferable while injecting detergent (as slow as possible) [31, 33, 56, 78].

I. SUMMARY OF THE STATE OF THE ART IN COMPRESSOR FOULING, DETECTION, AND LOCALIZATION

Based on an extensive review of the open literature, the following is a summary of the state of the art on the effects of fouling on cascade aerodynamics, compressor performance, the detection of fouling using measured performance, and the ability to use these measurements to determine the location of fouling.

1. Increasing airfoil roughness, beyond a level where the roughness elements protrude through the viscous sub-layer, increases the skin friction and hence momentum boundary layer thickness, particularly on the suction sides of the airfoils. This results in higher total pressure loss and lower turning (high deviation).
2. Fouling degrades all aspects of compressor performance, including pressure ratio, mass flow, efficiency, stall margin, and usable flow range.
3. Direct measurements of compressor performance are superior to measurements of engine parameters in detecting and localizing compressor fouling.
4. The measurement of static pressure depression at a compressor inlet, which is an indicator of mass flow, appears to be one of the most sensitive measures of fouling. Compressor pressure ratio and efficiency are in order less sensitive measures. Finally, temperature ratio is poor indicator of fouling.
5. Influence coefficients, which indicate ratios of percentage changes in two parameters, have been shown to provide information on fouling location.

However, to the best knowledge of the author, no analysis has been published in the open literature that provides a basis for determining the most effective physical quantities to measure to detect and localize compressor fouling, which clearly accounts for the two most important physical influences of airfoil hydrodynamic roughness, namely the increase in profile total pressure loss and the increase in deviation, which reduces the blade element turning and hence stage work. It is the objective of this study to supply just such an analysis.

III. 3-STAGE COMPRESSOR MODEL

A. OVERVIEW

This chapter explains the development of a simple, meanline, aerothermodynamic model of a three-stage axial compressor. The model predicts the effect of fouling, imposed as an increase in surface roughness, on the fouled stage, upstream stages, downstream stages, and on the overall performance of the three-stage compressor.

The model was written as a simple spreadsheet. The geometry of the compressor was chosen to approximate the inlet guide vanes and the first three stages of the Allison 501 compressor. It was a 'first-order' prediction of the trend of performance degradation due to fouling at different compressor stages.

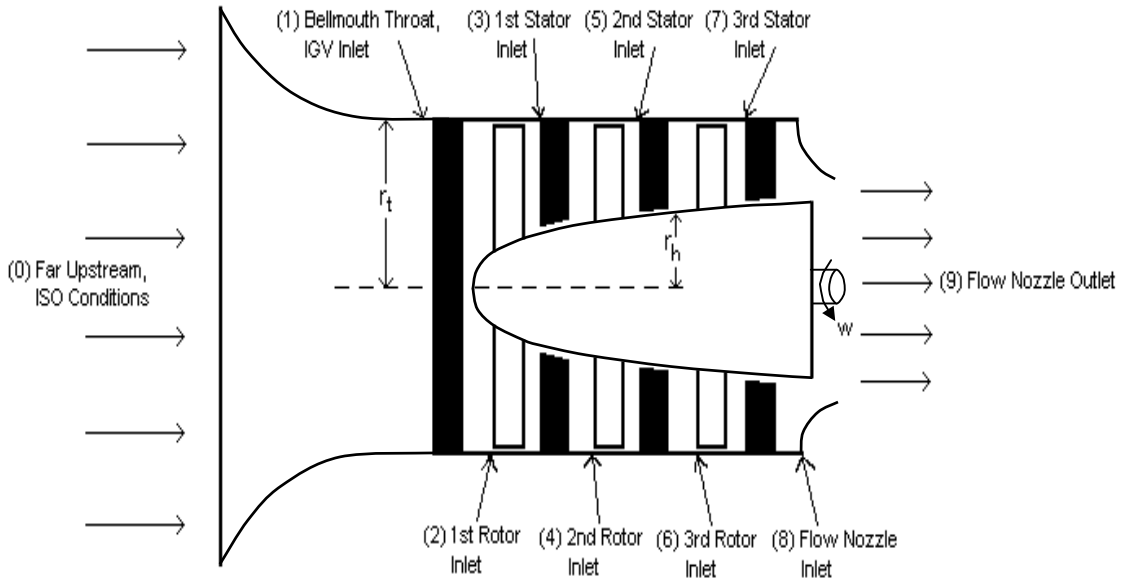

Figure 1. Three-Stage Compressor Model Schematic

B. MODEL ASSUMPTIONS

In the development of this model the following assumptions were used:

1. Ambient conditions were taken to be ISO conditions (P=101,325 Pa and T=15°C, 288.15 K).

2. Constant specific heat (C_p=1.004 kJ/kg-K) and ratio of specific heats

($\gamma = C_p/C_v = 1.4$) was assumed for air.

3. The gas constant for air was assumed to be constant (R=287 J/kg-K).
4. The kinematic viscosity of air was assumed constant at $1.47 \cdot 10^{-5}$ m^2/s.
5. Meanline analysis – the characteristics of the streamline at mid-span was calculated.
6. All airflow velocity profiles were assumed 2-dimensional and uniform.
7. Axisymmetric flow was assumed at the inlet to the bellmouth.
8. Adiabatic

C. GEOMETRIC BASELINE

Airfoil profile geometry varies significantly in the first three Allison 501-K compressor stages. The first two rotors have relatively low camber ($\gamma \cong 23°$) and stagger ($\lambda \cong 26°$). The third stage has increased camber and stagger. Since the lightly-cambered inlet guide vanes impart very little swirl on the inlet air stream, the first few stages operate at very 'high' flow coefficients at design inlet mass flow ($\phi \cong 0.9$, typical 1940s design [17]). To facilitate the analysis, NACA 65(12)10 series blades were used throughout the model and airfoil staggers were adjusted to attain more 'traditional' flow coefficients ($\phi \cong 0.65$). The following table displays the baseline geometry.

Table 1. Three-Stage Compressor Geometry

	IGV	**Rotor 1**	**Stator 1**	**Rotor 2**	**Stator 2**	**Rotor 3**	**Stator 3**
Tip Radius, r_t [m]	0.1868	0.1868	0.1868	0.1868	0.1868	0.1868	0.1868
Hub Radius, r_h [m]	0.0553	0.0553	0.0701	0.0849	0.0940	0.1030	0.1120
Mean Radius [m]	0.1378	0.1378	0.1411	0.1451	0.1479	0.1508	0.1540
Blockage (estimated)	0 %	0 %	1 %	2 %	3 %	4 %	5 %
Effective Annulus Area [m^2]	0.1000	0.1000	0.0932	0.0852	0.0794	0.0732	0.0667
Chord, C [m]	0.03	0.03	0.03	0.03	0.03	0.03	0.03
Max Thickness [m]	0.003	0.003	0.003	0.003	0.003	0.003	0.003
Solidity, S	1	1	1	1	1	1	1
Camber, γ [deg]	20	30	30	30	30	30	30
Stagger, λ [deg]	10.0	34.1	26.7	33.3	29.5	33.6	31.1

The annulus area was decreased through the compressor by increasing the hub radius. The area entering each, successive rotor and stator row was reduced so the axial velocity remained approximately constant through the compressor ($C_z \cong 136.7$ m/s). The inlet guide vanes were staggered for zero incidence. Rotor and stator staggers, λ_r and λ_s, were adjusted to attain two degrees of positive incidence for all rows at the baseline, clean condition. The geometry remained constant throughout all simulations.

D. CALCULATION OF CLEAN, BASELINE PERFORMANCE

1. Overview

Allison 501-K performance was modeled at ISO ambient conditions. For a clean compressor at a constant shaft speed of N=14,340 RPM, this corresponds to an air mass flow of approximately 15.377 kg/s (34.4 lbm/s) and a compression ratio of 12.5. A throttle was placed downstream to backpressure the stages to obtain the correct incidence and mass flow (i.e. the same as design).

Velocity triangles are often used to represent airflow angle and velocity entering and leaving compressor blade rows. Angles are measured from axial. Absolute velocities and angles are depicted by $\vec{C}$ and α, respectively. Rotor relative velocities and angles are labeled $\vec{W}$ and β, respectively. Assuming constant axial velocity and no radial motion, inlet and outlet velocity triangles can be overlaid.

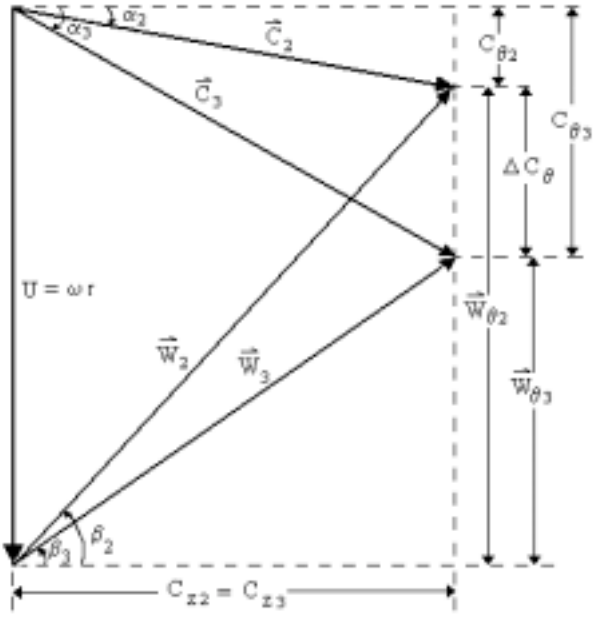

Figure 2. Velocity Triangle for the 1st Stage Rotor

2. Inlet Air

a. Bellmouth

Point (0) is assumed to be well upstream of the bellmouth, where static temperature equals total temperature and static pressure equals total pressure. Air density is assumed to be 1.225 kg/m^3. The bellmouth radius goes from 0.3810 m at point (0) to 0.1868 m at the point (1), the throat. The discharge coefficient is assumed to be 0.98. Total temperature and pressure are assumed to be constant across the bellmouth. The static pressure at the throat must be calculated. Since the Mach number at the throat is about 0.4, a form of the compressible flow equation is utilized to account for the reduction in density across the bellmouth. Accordingly,

$$\dot{m}_a = C_D \rho_1 A_1 c_{z1} = \frac{C_D P_{T1} A_1}{\sqrt{R T_{T1}}} \left(\frac{P_1}{P_{T1}} \right)^{\frac{1}{\gamma}} \sqrt{\frac{2\gamma}{\gamma - 1} \left(1 - \left(\frac{P_1}{P_{T1}} \right)^{\frac{\gamma - 1}{\gamma}} \right)} \tag{12}$$

is solved for P_1. Mass flow is initially assigned the design value of 15.377 kg/s in an empty cell on the 'Bellmouth' EXCEL worksheet. Mass flow will later be iterated through the compressor to the nozzle so the compressor adjusts the inlet mass flow during fouling scenarios.

The bellmouth is assumed to be nearly isentropic, so the static throat temperature is calculated by

$$T_1 = T_{T1} \left(\frac{P_1}{P_{T1}} \right)^{\gamma - 1 / \gamma} \tag{13}$$

The ideal gas law is used to determine the density at the throat by

$$\rho_1 = \frac{P_1}{R T_1} \tag{14}$$

and the inlet axial velocity is calculated from

$$\dot{m}_a = \rho_1 A_1 c_{z1} \tag{15}$$

As a final calculation at the throat, the Mach number at point (1) if found from

$$M_1 = \frac{c_{z1}}{\sqrt{\gamma R T_1}} \tag{16}$$

b. Inlet Guide Vanes

The inlet guide vanes impart a small amount of turning on the inlet air prior to entering the first stage. There is a small total pressure loss across the guide vanes. In the absence of empirical loss data for the very thin, lightly cambered 501-K inlet guide vane profile, the total pressure loss coefficient was assumed to be 0.02, where

$$\varpi = \frac{P_{T1} - P_{T2}}{P_{T1} - P_1} \tag{17}$$

for compressible flow. Total pressure at the guide vane outlet was calculated by

$$P_{T2} = P_{T1} - \varpi(P_{T1} - P_1) \tag{18}$$

The absolute air inlet angle (α_1) is from axial. The outlet air does not follow the extended mean camber line. There is a certain amount of mean flow deviation associated with an airfoil. Since the inlet guide vanes are staggered for zero incidence, the deviation angle is subtracted from the camber to find the outlet absolute flow angle. Deviation angle, δ_c, was calculated with Carter's Rule [17]:

$$\delta_C = m\gamma\left(\frac{s}{C}\right)^n \tag{19}$$

where n = 1 for IGVs and n = 0.5 for cascades. Carter's empirical deviation constant 'm' was obtained for the NACA-65(12)10 circular arc airfoils from Figure 3.

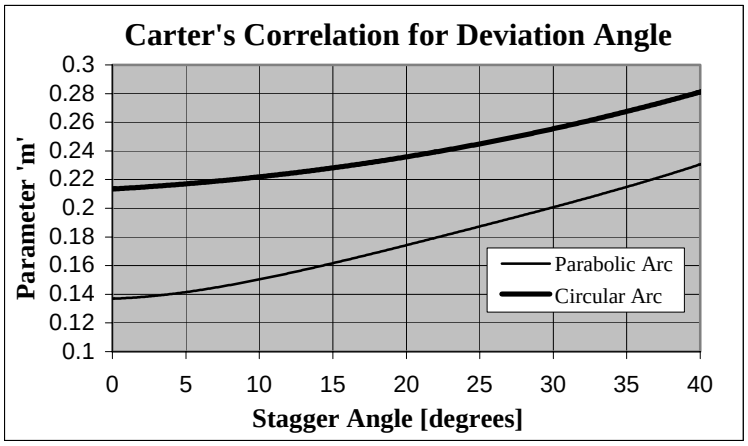

Figure 3. Deviation Angle by Carter's Rule [17]

It was assumed the axial velocity is constant through the row, so

$$C_2 = C_1 \frac{\cos(\alpha_1)}{\cos(\alpha_2)} \tag{20}$$

Total temperature is 288.15 K at point (2). The Mach number was first calculated by Equation (16) using total temperature to find the static temperature with

$$T_2 = \frac{T_{T2}}{1+\left(\frac{\gamma-1}{2}\right)M_2^{\,2}} \tag{21}$$

then refined by iteration to find T_2. Lastly, static pressure was calculated with

$$P_2 = \frac{P_{T2}}{\left(1+\frac{\gamma-1}{2}M_2^{\,2}\right)^{\gamma/\gamma-1}} \tag{22}$$

The IGV outlet conditions are the first stage rotor inlet conditions.

3. Stage Calculations

a. Rotor

The first stage rotor calculations will now be described, although the method and equations are the same for all three rotors. The relative and absolute velocities and angles of the airflow at the entrance and exit of the first stage rotor were calculated from Figure 2. Constant axial velocity is assumed across the rotor. The

relative inlet and outlet angles were checked with the appropriate turning chart [35] to ensure symmetric loading. The rotor deviation was estimated with Carter's Rule [17].

The relative inlet Mach number for the rotor was found by

$$M_{2,rel} = \frac{W_2}{\sqrt{\gamma R T_2}} \tag{23}$$

The relative inlet temperature and pressure was found by

$$T_{T2,rel} = T_2\left(1 + \frac{\gamma - 1}{2} M_{2,rel}{}^2\right) \tag{24}$$

and

$$P_{T2,rel} = P_2\left(1 + \frac{\gamma - 1}{2} M_{2,rel}{}^2\right)^{\frac{\gamma-1}{\gamma}} \tag{25}$$

respectively. The total pressure loss coefficient, ϖ, was initially assumed to be 0.02 for a smooth airfoil. The relative airflow Mach number for all airfoils was approximately 0.6.

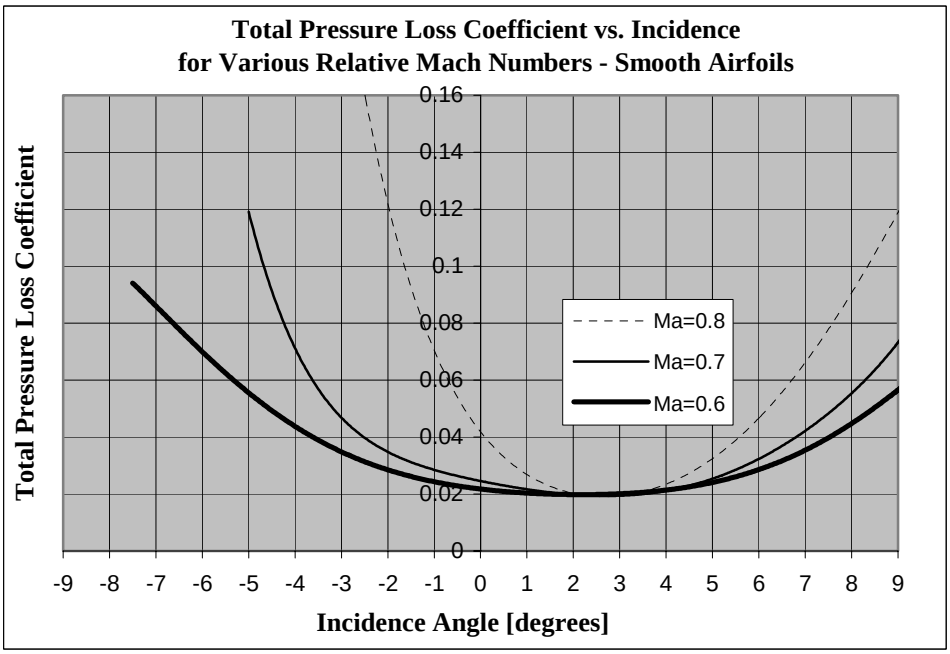

Figure 4. Total Pressure Loss Coefficient [57]

The initial mean roughness height for the clean rotor airfoils was assumed to be k = 3 μm. This resulted in a Reynolds number for the clean airfoil roughness

elements of $\mathrm{Re}_k \cong 43$. As explained in the Introduction, the blade was hydrodynamically smooth in the clean condition because $\mathrm{Re}_k << 100$.

The outlet relative total pressure is the inlet minus the loss in total pressure:

$$P_{T3} = P_{T2,rel} - \varpi(P_{T2,rel} - P_2) \tag{26}$$

Noting that $T_{T2,rel} = T_{T3,rel}$, the outlet relative Mach number was estimated by

$$M_{3,rel} \cong \frac{W_3}{\sqrt{\gamma R T_{T3,rel}}} \tag{27}$$

The initial estimate was used to find the first approximation of outlet static temperature:

$$T_3 = \frac{T_{T3,rel}}{\left(1 + \frac{\gamma - 1}{2} M_{3,rel}{}^2\right)} \tag{28}$$

With the Equations (27) and (28), T_3 was used to improve the approximation of $M_{3,rel}$, which was finally used to calculate the iterated value of T_3.

The work was calculated from Euler's Turbine Equation:

$$w = U\left(C_{\theta 3} - C_{\theta 2}\right) = c_p\left(T_{T3,abs} - T_{T2,abs}\right) \tag{29}$$

Hence, the absolute exit temperature, T_{T3}, was calculated. The exit absolute Mach number is approximately

$$M_{3,abs} = \frac{C_3}{\sqrt{\gamma R T_3}} \tag{30}$$

The isentropic total pressure (without losses) is

$$P_{T3s} = P_{T2}\left(\frac{T_{T3}}{T_{T2}}\right)^{\frac{\gamma}{\gamma - 1}} \tag{31}$$

The actual total exit pressure is

$$P_{T3} = P_{T3s} - \Delta P_{loss} \tag{32}$$

where $$\Delta P_{loss} = P_{T2,rel} - P_{T3,rel} \quad (33)$$

The exit static pressure was finally found from the absolute exit Mach number and total pressure:

$$P_3 = \frac{P_{T3,abs}}{\left(1 + \frac{\gamma - 1}{2} M_{3,abs}{}^2\right)^{\frac{\gamma}{\gamma - 1}}} \quad (34)$$

The rotor flow and pressure coefficients are calculated by

$$\phi = \frac{c_z}{U} \quad (35)$$

and $$\psi = \frac{\Delta C_\theta}{U} \quad (36)$$

respectively.

The airflow is subjected to an area change between the rotor outlet and stator inlet. Therefore, the compressible flow equation was used to account for changes in area, density, static pressure and static temperature (see previous section on 'Bellmouth' for the equation). Total temperature was assumed constant (no losses between the rotor and stator). To set the conditions at the first stage stator inlet, the spreadsheet iterates P_3 in the compressible flow equation (with a 'macro' in Visual Basic) until the mass flow equals the mass flow at the bellmouth, $\dot{m}_1 = \dot{m}_3$. The tolerance was set at +/- 0.01% for continuity of mass flow. Next, the static pressure at the first stage stator inlet was calculated from the isentropic relationship,

$$T_3 = T_{T3}\left(\frac{P_3}{P_{T3}}\right)^{\gamma - 1/\gamma} \quad (37)$$

Density was found by the ideal gas law, Equation (14). Lastly, the axial velocity was calculated from Equation (15). These conditions were applied to the first stage stator inlet.

b. Stator

The first stage stator calculations will now be described, although the method and equations are the same for all three stators. The stator calculations were carried out in the same manner as the IGVs with several differences. Because the stators and rotors have the same geometry, the same turning chart was used to ensure symmetric loading [35]. The initial mean roughness height for the clean stator airfoils was assumed to be the same as the rotors (k = 3 μm). The clean stator Reynolds number for the roughness elements was $\mathrm{Re}_k \cong 34$ (hydrodynamically smooth). As with the rotor, the first stage stator Mach number was approximately 0.6, so the same curve on Figure 4 was used to estimate the total pressure loss coefficient, ϖ. The stator deviation was estimated with Carter's Rule [17]. As was done in the rotor calculations, the spreadsheet was designed to carry out the same iterative loop (with a 'macro') to correct the inlet conditions for the second stage rotor for the area reduction.

c. Stage Performance

The first stage pressure and temperature ratios were calculated with

$$\pi_1 = \frac{P_{T4}}{P_{T2}} \tag{38}$$

and

$$\tau_1 = \frac{T_{T4}}{T_{T2}} \tag{39}$$

respectively. The stage efficiency is

$$\eta_1 = \frac{\pi_1^{\frac{\gamma-1}{\gamma}} - 1}{\tau_1 - 1} \tag{40}$$

This efficiency accounts for the loss measured in cascades, or profile loss (predicted by the model), as well as other losses, such as annulus and secondary losses. It is common to quote the estimate for the different losses given by Howell in 1945 [17], shown here as Figure 5. In the region of design flow coefficient (about 0.60 to 0.66 for this 3-stage compressor), annulus and secondary losses may be considered constant. Howell's loss relationship attributes 39% of stage efficiency loss to profile (cascade) losses, 41% to secondary losses, and 20% to annulus losses. Tip loss was not included. When

correlated to Howell's loss relationship, the estimated stage efficiencies for this 3-stage compressor model (Profile+Secondary+Annulus Loss) fit the curve within +/- 0.14%.

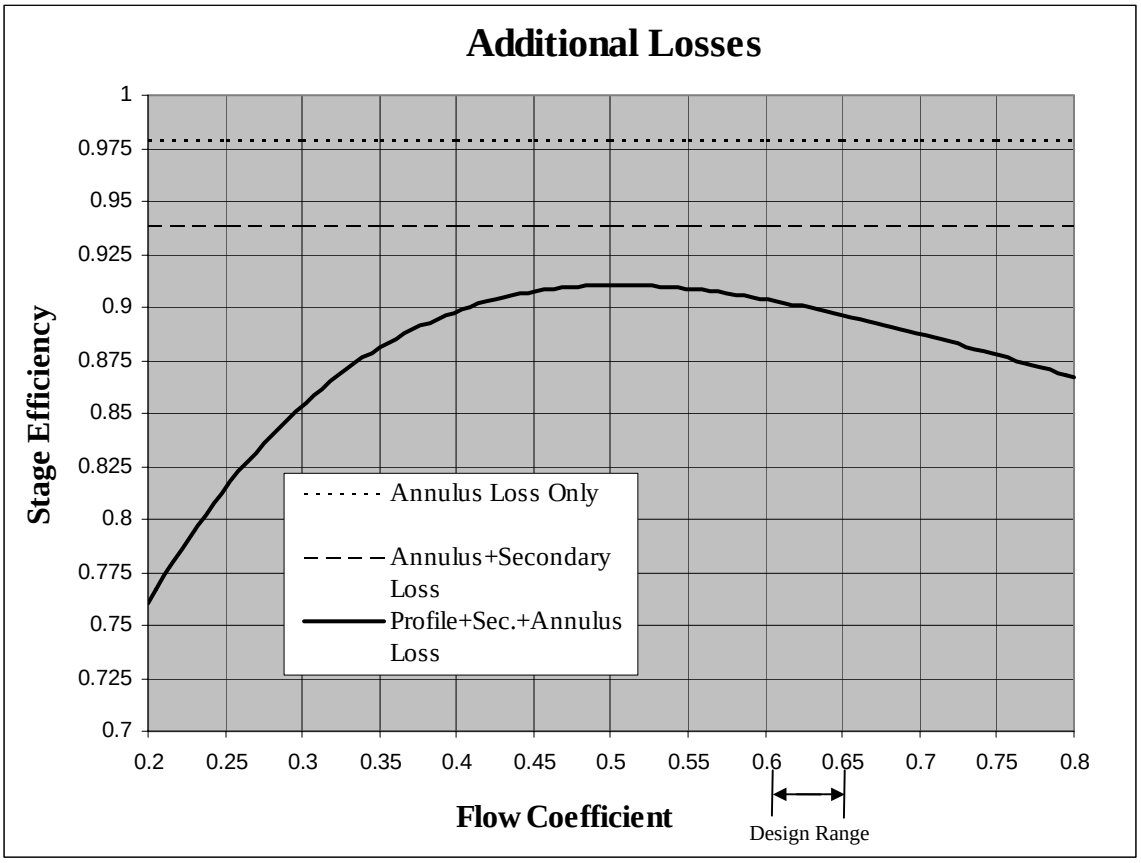

Figure 5. Howell's Estimate of Additional Losses [17]

d. Throttle Calculations

The rotor and stator calculations for each stage proceed through the compressor, maintaining continuity of mass flow, until the third stage outlet is reached (point (8) on Figure 1). A simple flow nozzle [39] was introduced at the third stage exit to backpressure the 3-stage compressor, enabling it to take in the design mass flow. The throttle discharges to ambient conditions at point (9), which are at the same ISO conditions as point (0). The mass flow through the throttle is

$$\dot{m}_{a,throttle} = \left(\frac{C_d A_{throat} Y}{\sqrt{1-\beta^4}} \right) \sqrt{2\rho_8 (P_8 - P_{T9})} \tag{41}$$

The discharge coefficient, C_D, was assumed to be 1 (no loss). The throat area, A_{throat}, is the area at the throat of the nozzle, β is the diameter ratio, where $\beta = D_{throat} / D_8$, and Y is the expansion factor to account for compressibility, where

$$Y = \sqrt{\frac{(1-\beta^4)\left(\left(\frac{P_{T9}}{P_{T8}}\right)^{2/\gamma} - \left(\frac{P_{T9}}{P_{T8}}\right)^{\gamma+1/\gamma}\right)}{\left(\frac{\gamma-1}{\gamma}\right)\left(1-\frac{P_{T9}}{P_{T8}}\right)\left(1-\beta^4\left(\frac{P_{T9}}{P_{T8}}\right)^{2/\gamma}\right)}} \tag{42}$$

The diameter of the orifice was adjusted until the mass flow through the nozzle equaled the mass flow into the compressor at the bellmouth (remember, the bellmouth is still set at $\dot{m}_{a,design}$ = 15.377 kg/s).

e. Making the Model Interactive

EXCEL 'macros' solve for compressible flow with area reduction from the bellmouth to the third stage exit, which maintains continuity of flow throughout the 3-stage compressor. The throttle now needs to be adjusted so that the compressor actually 'sucks' 15.377 kg/s. The calculation mode for the cell on the Bellmouth worksheet that indicates mass flow (currently set for 15.377 kg/s) is changed to "Iteration". While the cell is highlighted, press "=" and page to the 'Throttle' worksheet and click on the cell that calculates $\dot{m}_{a,throttle}$ (links together the inlet and outlet). While in this iterative mode, the spreadsheet automatically adjusts so that it takes in the same mass flow that leaves through the throttle.

The 'macro' that iterates the compressible flow equation between the rotors and stators (5 different iterations running separately) now needs to be run to make mass flow continuous throughout the compressor. The five iterations run separately 4-5 times, inside the continuous iteration loop that ensures $\dot{m}_1 = \dot{m}_{a,throttle}$, until the specified tolerance for mass flow error is met. For this case, tolerance for mass flow error was set at +/-0.01% throughout. On a Pentium-IV processor, this took about 3-4 minutes to run.

After running the program the mass flow is of course not equal to 15.377 kg/s. However, the spreadsheet is fully interactive and the nozzle orifice gap may be adjusted and the 'macro' is then re-run until 15.377 kg/sec is attained. At that point, the 3-stage compressor model is base-lined for the clean condition.

E. CALCULATION OF FOULED, OFF-DESIGN PERFORMANCE

1. Overview

Fouling was introduced in the form of added roughness to the first stage baseline, and the simulation was run with only the first stage roughened. Next, fouling was introduced as added roughness to the second stage baseline, and the simulation was run with only the second stage roughened. Lastly, fouling was introduced as added roughness to the third stage baseline, and the simulation was run with only the third stage roughened.

Roughness elements were not actually 'placed' on the airfoils. A level of roughness was added uniformally to the airfoil surfaces that was assumed to double the total pressure loss coefficient, ϖ, and increase the deviation, δ_s, according to Shakhov's [41] relationship. Shakhov's deviation rule is described in Section 5, "Increase in Deviation". Besides the roughness, the geometry remained constant (Table 1) for all runs.

2. Imposing a Level of Roughness to Double ϖ

As described in the previous section, the mean roughness height for the clean, smooth airfoils was assumed to be k = 3 μm. The corresponding roughness parameter was found to be $C/k = 10{,}000$ for the clean airfoils. The rotor and stator Reynolds numbers were calculated by

$$\mathrm{Re}_{rotor} = \frac{\vec{W}\mathrm{C}}{\nu} \tag{43}$$

and

$$\mathrm{Re}_{stator} = \frac{\vec{C}\mathrm{C}}{\nu} \tag{44}$$

The rotor Reynolds number was approximately $\mathrm{Re}_{rotor} \cong 430{,}000$, and the stator Reynolds number was approximately $\mathrm{Re}_{stator} \cong 340{,}000$, for all stages. With these values

of airfoil Reynolds number and roughness parameter, the flat-plate analog of the Moody diagram [88] was used to estimate the drag coefficient, C_D. It was found that $C_D \cong 0.004$.

It was assumed that doubling the drag coefficient, $C_{D,}$ is similar to doubling the total pressure loss coefficient, ϖ. Doubling the drag coefficient made $C_D \cong 0.008$, which corresponds to an approximate roughness parameter of $C/k = 1{,}000$ on the Moody diagram [88]. With a standard chord length, C, of 0.03 m, the resulting mean roughness height was k = 30 μm, or ten times the initial, smooth airfoil roughness height. The Reynolds number of the roughness elements for the fouled airfoils was $\mathrm{Re}_k \cong 430$ for rotors and $\mathrm{Re}_k \cong 340$ for stators. As explained in the Introduction, the uniformally roughened blades were hydrodynamically rough because $\mathrm{Re}_k >> 100$, meaning the roughness elements protruded well into the viscous sublayer.

3. Increase in Deviation

The reduction in airfoil turning (work) due to added roughness was accounted for by an increase in deviation, δ, by Shakhov's [41] equation. As described in the Introduction, Shakhov's experiments produced an equation to calculate deviation that accounts for the mean height of the roughness elements, incidence and solidity. Figure 6 compares the deviation found by several methods for airfoils with 30 degrees of camber and solidity of 1.25.

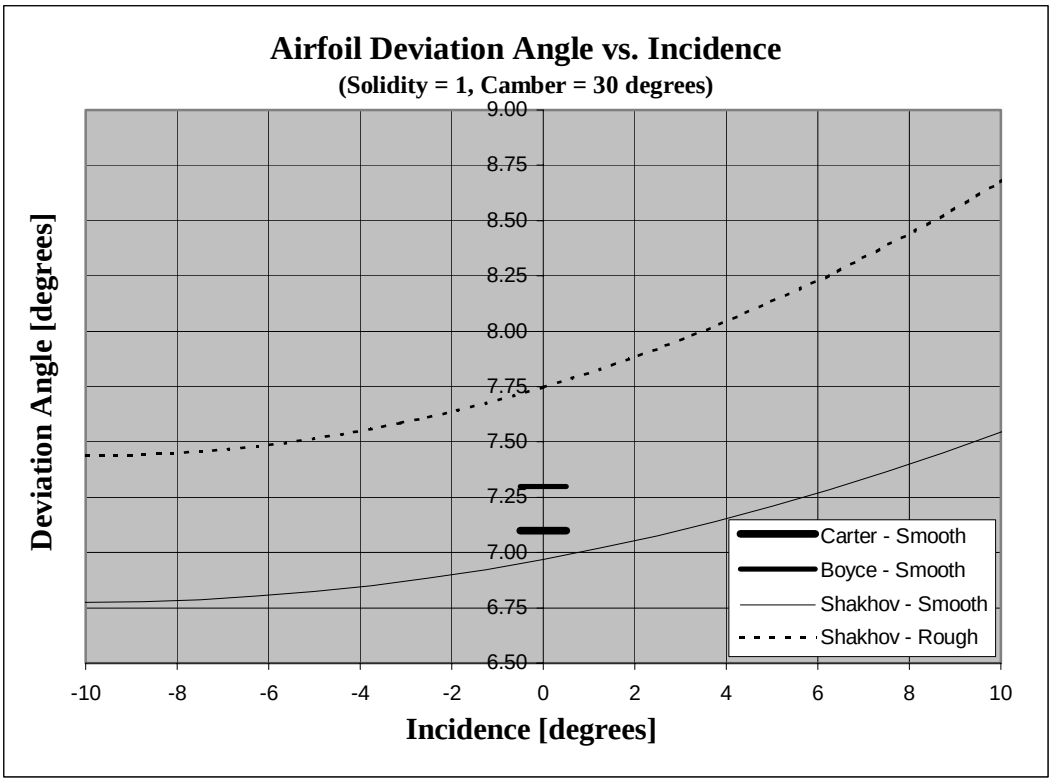

Figure 6. Airfoil Deviation Angle by Various Methods [10, 17, 41]

The increase in deviation for the roughened airfoils varied between 3-4% for rotors and 8-10% for stators. Shakhov's paper [41] was the only quantitative information found on the effect of airfoil roughness on deviation angle. Shakhov's experiments were conducted on airfoils of slightly less camber (28 degrees) and lower Reynolds numbers of ~ 250,000. Although the experimental conditions were not exactly the same as for this simulation, the formula was a relationship that produced the expected increase in deviation for all fouling cases; the trends are correct and that was deemed most important for this first order approximation.

4. Fouling Simulations

For the first model simulation, the first stage rotor and stator were roughened uniformally. As described in the previous two sections, this affected the first stage by doubling the total pressure loss and increasing the deviation. The total pressure loss coefficient and deviation for stage 2 and stage 3 was estimated from Figure 4 and Carter's Rule, as was done for the baseline, clean condition. All other calculations were performed as previously described for the clean condition.

The ‘macro’ was run for the fouled first stage condition and the results were examined to see the effect on performance of the first stage, second stage, third stage, and overall compressor performance. The same procedure was conducted for uniform roughening of the second stage rotor and stator, then finally for the third stage. The effects of fouling of equal magnitude at various locations within the 3-stage compressor model were analyzed and are presented in Chapter IV.

IV. SIMULATION RESULTS

A. FIRST STAGE FOULING

1. Results

Table 2 presents the effect of uniform first stage fouling on the performance of each individual stage. Stages 2 and 3 are clean.

Table 2. Compressor Model Stage Performance, First Stage Fouled

	STAGE 1		**STAGE 2**		**STAGE 3**	
	CLEAN	**FOULED**	CLEAN	FOULED	CLEAN	FOULED
Rotor Incidence, *i* [degrees]	**2.00**	**2.57**	2.00	1.61	2.00	1.84
Axial Velocity, C_z [m/s]	**136.68**	**134.43**	136.69	136.27	136.70	136.62
Flow Coeff., ϕ	**0.661**	**0.650**	0.627	0.625	0.603	0.603
Pressure Coeff., ψ	**0.449**	**0.440**	0.417	0.411	0.402	0.400
Pressure Ratio, π	**1.242**	**1.227**	1.233	1.230	1.228	1.227
Temperature Ratio, τ	**1.066**	**1.065**	1.064	1.063	1.063	1.063
Efficiency, η	**90.02%**	**86.12%**	90.02%	89.98%	90.05%	90.04%

2. Effect of First Stage Fouling on Each Stage

Fouling of the first stage increased the total pressure loss across the blade rows and reduced the effective flow area. The reduction in flow area due to boundary layer growth, and the greater rate of entropy production, which decreased the stagnation density, decreased the compressor mass flow, $\dot{m}_a$. The reduction in mass flow greatly reduced the axial velocity into the first stage, C_{z2}, and flow coefficient, ϕ_2, pushing the first stage rotor to greater positive incidence, i. The reduction in mass flow also reduced the axial velocity and flow coefficient into the downstream stages. However, the growth of the momentum boundary layer in the first stage caused an increase in flow deviation angle, which meant a reduction in turning. The reduction in turning in the first stage pushed the downstream stages to negative incidence, and tended to increase the axial velocity. As a result, the downstream stages showed only a slight decrease in axial velocity and flow coefficient.

The reduction in turning by the first stage, and the reduction of work in the first stage rotor, resulted in a decrease in the first stage pressure (work) coefficient, ψ_{st}. The reduction of positive incidence on the downstream stages increased the total pressure loss slightly (see Figure 4). Carter's Rule (Equation 19) does not account for the decrease of incidence on the downstream, clean stages in calculating deviation. Therefore, an additional, slight reduction in turning in the downstream stages occurred. The result was a minor reduction in the pressure coefficient in the downstream stages.

A doubling of the total pressure loss coefficient and increase in deviation in the first stage reduced the first stage pressure ratio, π_{st}, by about 1.2%. The downstream stages exhibited a slight reduction in pressure ratio. The temperature ratio, τ_{st}, of the fouled first stage, and clean downstream stages, all decreased slightly (~ 0.10%).

The decrease in turning and work in the first stage rotor, and a reduction of turning in the stator, reduced the first stage efficiency, η_{st}, by about 4%. There was only a very slight reduction in turning and specific work in the downstream stages, hence a 0.04% and 0.01% reduction in efficiency was seen in the second and third stage, respectively.

B . SECOND STAGE FOULING

1. Results

Table 3 presents the effect of uniform second stage fouling on the performance of each individual stage. Stages 1 and 3 are clean.

Table 3. Compressor Model Stage Performance, Second Stage Fouled

	STAGE 1		**STAGE 2**		**STAGE 3**	
	CLEAN	FOULED	**CLEAN**	**FOULED**	CLEAN	FOULED
Rotor Incidence, *i* [degrees]	2.00	2.55	**2.00**	**2.43**	2.00	1.61
Axial Velocity, C_z [m/s]	136.68	134.78	**136.69**	**134.73**	136.70	136.43
Flow Coeff., ϕ	0.661	0.652	**0.627**	**0.619**	0.603	0.603
Pressure Coeff., ψ	0.449	0.449	**0.417**	**0.407**	0.402	0.396
Pressure Ratio, π	1.242	1.242	**1.233**	**1.217**	1.228	1.225
Temperature Ratio, τ	1.066	1.066	**1.064**	**1.063**	1.063	1.062
Efficiency, η	90.02%	90.08%	**90.02%**	**86.09%**	90.05%	90.02%

Velocity triangles, which express the effect of uniform second stage fouling on the performance of each individual stage, are presented in Figure 7. Stages 1 and 3 are clean. Solid lines are for the "clean" condition and dotted lines are for the condition of the second stage fouling (also labeled with the subscript, *f*, meaning fouled). While the subscripts are for fouling of the second stage, Figure 7 may also used to describe the velocity triangles due to a typical imbedded stage. For example, the first stage velocity triangles for fouling of the first stage look like the middle diagram, entitled "Fouled Stage". Similarly, for first stage fouling, the second and third stage velocity triangles look like the diagram on the right, entitled "Downstream Stage".

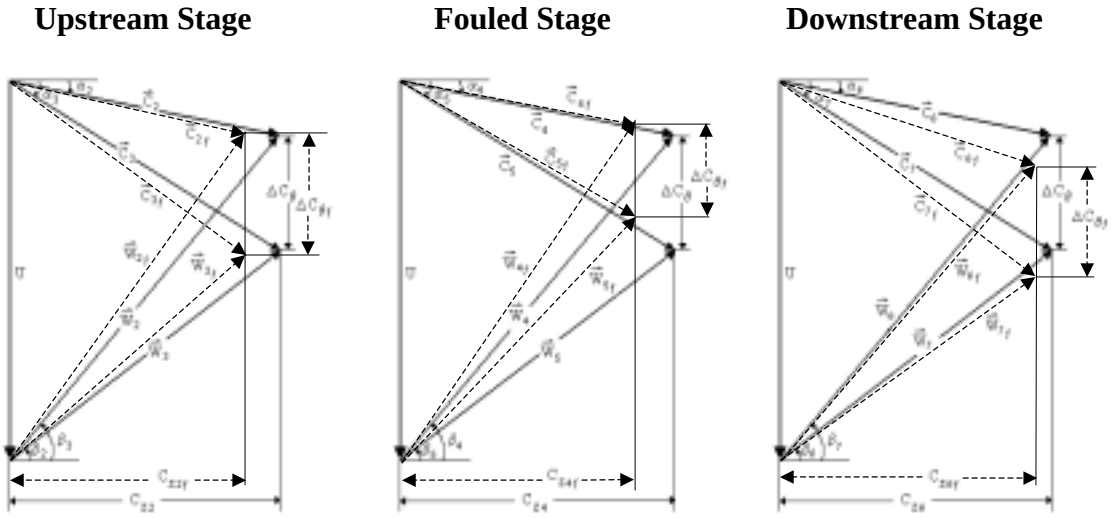

Figure 7. Approximate Velocity Triangles for Second Stage Fouling

2. Effect of Second Stage Fouling on Each Stage

Fouling of the second stage increased the total pressure loss across the blade rows and reduced the effective flow area. The reduction in flow area due to boundary layer growth, and the greater rate of entropy production, which decreased the stagnation density, decreased the compressor mass flow. The reduction in mass flow greatly reduced the axial velocity and flow coefficient into the first and second stages, pushing the upstream stage and the fouled stage to greater positive incidence. The reduction in mass flow also reduced the axial velocity and flow coefficient into the downstream stage. However, the growth of the momentum boundary layer in the second stage caused an

increase in flow deviation angle, which meant a reduction in turning. The reduction in turning in the second stage pushed the downstream stage to negative incidence, and tended to increase the axial velocity. As a result, stage 3 showed only a slight decrease in axial velocity and flow coefficient.

The reduction in turning by the second stage, and the reduction of work in the second stage rotor, resulted in a decrease of the second stage pressure (work) coefficient. The reduction of positive incidence on stage 3 increased the total pressure loss slightly (see Figure 4). Carter's Rule (Equation 19) does not account for the decrease of incidence on the downstream, clean stage in calculating deviation. Therefore, an additional, slight reduction in turning in the downstream stage occurred. The result was a minor reduction in the pressure coefficient for stage 3. The first stage was pushed to greater positive incidence, while the total pressure loss remained constant (Figure 4). Therefore, the upstream stage pressure coefficient remained constant.

A doubling of the total pressure loss coefficient and increase in deviation in the second stage reduced the second stage pressure ratio by about 1.3%. The downstream stage exhibited a slight reduction in pressure ratio and the upstream stage remained constant. The temperature ratio of the fouled second stage, and clean downstream stage, both decreased slightly (~ 0.10%). The temperature ratio of the upstream stage remained constant.

The decrease in turning and work in the second stage rotor, and the reduction of turning in the stator, reduced the second stage efficiency by about 4%. There was only a very slight reduction in turning and specific work in the downstream stage, hence the third stage exhibited a 0.03% reduction in efficiency. The increase in positive incidence seen by the upstream stage resulted in a 0.06% increase in first stage efficiency.

C. THIRD STAGE FOULING

1. Results

Table 4 presents the effect of uniform third stage fouling on the performance of each individual stage. Stages 1 and 2 are clean.

Table 4. Compressor Model Stage Performance, Third Stage Fouled

	STAGE 1		STAGE 2		STAGE 3	
	CLEAN	FOULED	CLEAN	FOULED	**CLEAN**	**FOULED**
Rotor Incidence, i [degrees]	2.00	2.47	2.00	2.37	**2.00**	**2.33**
Axial Velocity, C_z [m/s]	136.68	135.10	136.69	135.05	**136.70**	**135.09**
Flow Coeff., ϕ	0.661	0.653	0.627	0.620	**0.603**	**0.597**
Pressure Coeff., ψ	0.449	0.449	0.417	0.416	**0.402**	**0.392**
Pressure Ratio, π	1.242	1.242	1.233	1.233	**1.228**	**1.212**
Temperature Ratio, τ	1.066	1.066	1.064	1.064	**1.063**	**1.061**
Efficiency, η	90.02%	90.07%	90.02%	90.06%	**90.05%**	**86.15%**

2. Effect of Third Stage Fouling on Each Stage

Fouling of the third stage increased the total pressure loss across the blade rows and reduced the effective flow area. The reduction in flow area due to boundary layer growth, and the greater rate of entropy production, which decreased the stagnation density, decreased the compressor mass flow. The reduction in mass flow reduced the axial velocity and flow coefficient into the first, second and third stages, pushing the upstream stages and the fouled stage to greater positive incidence.

The reduction in turning by the third stage, and the reduction of work in the third stage rotor, resulted in a decrease of the third stage pressure (work) coefficient. The first and second stages were pushed to greater positive incidence, while the total pressure losses remained constant (Figure 4). Therefore, the upstream stage pressure coefficients remained approximately constant.

A doubling of the total pressure loss coefficient and increase in deviation in the third stage reduced the third stage pressure ratio by about 1.3%. The pressure ratios for the upstream stages remained constant. The temperature ratio of the fouled third stage decreased slightly (~ 0.19%). The temperature ratios of the upstream stages remained constant.

The decrease in turning and work in the third stage rotor, and the reduction of turning in the stator, reduced the third stage efficiency by about 4%. The increase in

positive incidence seen by the upstream stages resulted in an increase in efficiency of 0.05% and 0.04% for the first and second stage, respectively.

D. OVERALL PERFORMANCE

1. Results

Table 5 presents the effect of fouling of each stage separately (3 simulations) on the overall compressor performance.

Table 5. Compressor Model Overall Performance

	CLEAN	1st Stage Fouled	% Change	2nd Stage Fouled	% Change	3rd Stage Fouled	% Change
Pressure Ratio, π_c	1.880	1.850	-1.575%	1.852	-1.517%	1.856	-1.274%
Temperature Ratio, τ_c	1.206	1.203	-0.219%	1.204	-0.213%	1.204	-0.151%
Efficiency, η_c	89.80%	88.38%	-1.58%	88.44%	-1.51%	88.51%	-1.43%
Mass Flow $\dot{m}_a$, [kg/s]	15.377	15.167	-1.367%	15.200	-1.147%	15.229	-0.958%
Intake Depression ΔP_{intake} , [Pa]	11,425	11,067	-3.14%	11,123	-2.64%	11,173	-2.21%

The compressor pressure ratio, π_c, was reduced 1.58% by first stage fouling, 1.52% by second stage fouling and 1.27% by third stage fouling. The compressor temperature ratio, τ_c, dropped 0.22% due to first stage fouling, 0.21% due to second stage fouling, and 0.15% due to third stage fouling.

Compressor efficiency, η_c, had only a slight dependence on fouling location. Overall efficiency reduced 1.58%, 1.51% and 1.43% due to fouling of the first, second and third stages, respectively. This corresponds to the fouling localization studies conducted by Zaba [91], where his fouling simulations showed very little dependence of compressor efficiency on fouling location.

The reduction in compressor mass flow, $\dot{m}_a$, reduced 1.37%, 1.15% and 0.96% for fouling of the first, second and third stages, respectively. The reduction in mass flow is therefore dependent on the location of fouling. This dependence agrees with Zaba's [91] theoretical work and field experiences, which showed a much greater reduction in mass flow for early stage fouling as compared to fouling of the latter stages.

Intake depression, ΔP_{intake}, proved to be the most sensitive parameter to monitor fouling regardless of its location in the compressor. Intake depression dropped 3.14%, 2.64% and 2.21% due to fouling of the first, second and third stages, respectively. The superior sensitivity of intake depression to fouling was demonstrated in several field applications by Scott [73] and Saravanamuttoo [69].

2. Influence Coefficients

Table 6 presents various influence coefficients, indicating ratios of percentage changes in two parameters due to fouling of each stage separately (3 simulations) on the overall compressor performance.

Table 6. Influence Coefficients for Overall Compressor Performance

Influence Coefficient	1st Stage Fouled	2nd Stage Fouled	3rd Stage Fouled
$I_{\dot{m}_a,\eta_c}$, $\frac{\%\Delta\dot{m}_a}{\%\Delta\eta_c}$	0.864	0.762	0.669
$I_{\dot{m}_a,\pi_c}$, $\frac{\%\Delta\dot{m}_a}{\%\Delta\pi_c}$	0.868	0.756	0.752
$I_{\dot{m}_a,\tau_c}$, $\frac{\%\Delta\dot{m}_a}{\%\Delta\tau_c}$	6.242	5.385	6.344
I_{η_c,π_c}, $\frac{\%\Delta\eta_c}{\%\Delta\pi_c}$	1.003	0.995	1.122
I_{π_c,τ_c}, $\frac{\%\Delta\pi_c}{\%\Delta\tau_c}$	7.192	7.122	8.437

An influence coefficient comparing the reduction in mass flow to the reduction in efficiency, $I_{\dot{m}_a,\eta_c}$, was seen to reduce significantly as the location of fouling moved from front to rear (~ 12% in reduction $I_{\dot{m}_a,\eta_c}$ per stage from as fouling location moved from stage 1 to 3). While the influence coefficient does not match Zaba's [91] results quantitatively, the trend is in agreement. Zaba conducted his simulations on a 16-stage compressor. If more stages were stacked onto this 3-stage model, the range of the influence coefficient, $I_{\dot{m}_a,\eta_c}$, due to fouling at various stages would likely increase significantly.

An influence coefficient comparing the reduction in mass flow to the reduction in pressure coefficient, $I_{\dot{m}_a,\pi_c}$, reduced significantly as the location of fouling moved from the first stage to the middle stage. However, the reduction in this influence coefficient between fouling at stage 2 and 3 was only about 0.5%. Therefore, $I_{\dot{m}_a,\pi_c}$ is not a good indicator of fouling location.

The remaining three influence coefficients, $I_{\dot{m}_a,\tau_c}$, I_{η_c,π_c} , and I_{π_c,τ_c} , all proved to be poor indicators of fouling location for this three-stage model. These influence coefficients all exhibited a decreasing trend between as fouling location moved from stage to stage 2. However, they all increased as fouling location moved from stage 2 to stage 3. Therefore, they were ineffective in localizing fouling.

V. SUMMARY, CONCLUSIONS AND RECOMMENDATIONS

A. SUMMARY

A study was conducted to explore the nature of compressor fouling, gain understanding of the state of the art in fouling detection, and investigate methods to measure and localize fouling. Several commonly used fouling detection techniques were examined, as well as a method to localize fouling by comparing several performance characteristics.

A computer model of the meanline flow in a 3-stage compressor was developed to simulate fouling by adding roughness at the first, middle, and rear stages, individually. The analysis included both an increase in total pressure losses and an increase in deviation in the fouled stage. It is believed that this is the first published work which included both. The simulations, though approximate regarding losses imposed and the increase in deviation on the fouled stages, exhibited trends in agreement with the literature.

B. CONCLUSIONS

The following conclusions were drawn from this study:

1) Compressor static pressure depression at the inlet, ΔP_{intake}, which is an indicator of mass flow, is the most sensitive parameter to monitor the degree of compressor fouling, regardless of location. However, it is a much more sensitive indicator of typical, early stage fouling. Intake depression was approximately twice as sensitive as any other parameter to indicate early stage fouling.

2) For uniform fouling of a single stage, the reduction in mass flow decreases steadily as the fouling location moves downstream. The reduction in compressor efficiency has a very slight dependence on fouling location. Hence, an influence coefficient, $I_{\dot{m}_a,\eta_c}$, comparing the percent reduction in mass flow to the percent reduction in efficiency, is the best to localize fouling. The reduction in $I_{\dot{m}_a,\eta_c}$ was approximately 12% per stage as fouling location moved downstream, which is a significant, measurable decrease.

C. RECOMMENDATIONS

The following recommendations are made for future work:

1) Model the full scale Allison 501-K 14-stage compressor with streamlines instead of an approximate, mean streamline taken at mid-span. Make predictions of the influence coefficient, $I_{\dot{m}_a,\eta_c}$.

2) Validate these theoretical predictions at the land based engineering site (LBES), or in the lab at the Naval Postgraduate School on the Allison C-250.

3) The compressor inlet and exit total pressure and temperature should be measured, along with the static pressure at the compressor inlet. These measurements would allow monitoring of compressor efficiency and the mass flow with intake depression for added roughness at various locations. Validate these theoretical predictions that the influence coefficient has a strong dependence on fouling location.

LIST OF REFERENCES

1. Abdelrazik, A. and Cheney, P., "Compressor Cleaning Effectiveness for Marine Gas Turbines", *Proceedings from the 1991 International Gas Turbine and Aeroengine Congress and Exposition*, June 1991, ASME Paper No. 91-GT-11.

2. Allison Engine Company, *501-K34 Installation Design*, Tech Manual, May 1989.

3. Antonazzi, Frank J., "Pressure Ratio Measurement Device", U.S. Patent #4,434,664.

4. Arnulfi, Gianmario L. and Massardo, Aristide F., "Effect of Axial Compressor Deterioration on Gas Turbines and Combined Cycle Power Plants", *Proceedings of the 7th Congress and Exposition on Gas Turbines in Cogeneration and Utility Industrial and Independent Power Generation*, Sep 1993, IGTI vol. 8.

5. Benvenuti, E. et al, "Gas Turbine Cycle Modeling Oriented to Component Performance Evaluation From Limited Design or Test Data", *IGTI Publication*, vol. 8, Cogen-Turbo Conference 1993.

6. Bammert, K. and Woelk, G. U., "The Influence of the Balding Surface Roughness on the Aerodynamic Behavior and Characteristic of an Axial Compressor", *Journal of Engineering for Power*, Transactions from ASME, vol. 102, no.2, Apr 1980.

7. Bouris, D et al, "Numerical Comparative Study of Compressor Rotor and Stator Blade Deposition Rates", *Proceedings of the ASME Turbo Expo 2002*, Jun 3-6.

8. Boyce, M.P. et al, "Condition Monitoring and Diagnostic Approaches for Advanced Gas Turbines", *IGTI Publication*, vol. 8, Cogen-Turbo Conference 1993.

9. Boyce, M.P., *Gas Turbine Engineering Handbook*, Gulf Publishing Co., 1995.

10. Boyce, M. P. et al, "Modeling and Analysis of Gas Turbine Performance Deterioration", *Journal of Engineering for Gas Turbines and Power*, vol. 116, ASME Paper 92-GT-395.

11. Boynton, J., "Investigation of Rotor Blade Roughness Effects on Turbine Performance", *Journal of Turbomachinery*, vol. 115, Jul 1993.

12. Brown, L., "Axial Flow Compressor and Turbine Loss Coefficients: A Comparison of Several Parameters", *Journal of Engineering for Power*, Jul 1972.

13. Caguiat, Daniel E. et al (Carderock Div.), "Compressor Fouling Testing On Rolls Royce/Allison 501-K17 and GE LM2500 Gas Turbine Engines", 2001.

14. Chow, Ronald et al, “Coatings Limit Compressor Fouling”, *Turbomachinery International*, Jan/Feb 1995.

15. Crosa, G et al, “Heavy-Duty Gas Turbine Aerothermodynamic Simulation Using Simulink”, *Proceedings of the 1996 ASME Turbo Asia Conference*, Nov 5-7, Jakarta, Indonesia.

16. Crosa, G.; Troila, M.; Torelli, A., “Turbine Model Improvement For a Heavy-Duty Gas Turbine Plant Simulation”, *Proceedings of the 1998 International Gas Turbine & Aeroengine Congress and Exhibition,* Jun 2-5, 1998, Stockholm, Sweden, ASME Paper # 98-GT-171.

17. Cumpsty, N.A., *Compressor Aerodynamics*, Longman Singapore Publishers, 1989.

18. Desideri, Umberto, “Performance Analysis of Gas Turbines Operating at Different Atmospheric Conditions”, *ASME IGTI Publication*, vol. 9, 1994, Oct**.** 25-27, 1994, Portland, OR.

19. Diakunchak, Ihor S., “Performance Deterioration in Industrial Gas Turbines”, *Proceedings from the 1991 International Gas Turbine and Aeroengine Congress and Exposition*, June 1991, ASME Paper No. 91-GT-228.

20. Dixon, S.L., *Thermodynamics of Turbomachinery*, Pergamon Press, 1978.

21. Doyle, M.D.; Dixon, S.L., “The Stacking of Compressor Stage Characteristics to Give an Overall Compressor Performance Map”, *Aeronautical Quarterly*, Nov 1962.

22. Eastman, J.M.; Thoman, D.C., “Fluidic Compressor Bleed Valve Control for Small Gas Turbine Engines”, *Fluidics Quarterly*, vol. 9, no. 3, Jul 1977, p.21-34.

23. Elmendorf, Wolfgang et al, “Three Dimensional Analysis of a Multi-Stage Compressor Flow Field”, *Proceedings of the 1998 International Gas Turbine & Aeroengine Congress and Exhibition*, Jun 2-5, 1998, Stockholm, Sweden, ASME Paper # 98-GT-249.

24. Escuret, J.F. and Elder, R.L., “Prediction and Active Control of Surge in Multi-Stage Axial-Flow Compressors”, *RFM, Revue Francaise de Mecanique*, no. 4, 1992.

25. Fetescu, Mircea, “Method and Apparatus for Keeping Clean and/or Cleaning a Gas Turbine Using Externally Generated Sound”, U.S. Patent #5,758,486.

26. Francis, George W. et al, “Applying Auxiliary Power Unit Technology to Starting Ship’s Gas Turbines”, *Proceedings of the 1991 International Gas Turbine & Aeroengine Congress and Exposition*, Jun 3-6, 1991, Orlando, FL.

27. Garnier, V.H. et al, “Rotating Waves as a Stall Indication in Axial Compressors”, *Journal of Turbomachinery*, vol. 113, no. 2 Apr 1991.

28. Garrard, Doug et al, “One Dimensional, Time Dependent Inlet/Engine Numerical Simulation For Aircraft Propulsion Systems”, *Proceedings of the 1997 International Gas Turbine & Aeroengine Congress and Exposition*, Jun 2-5, 1997, Orlando, FL, ASME Paper # 97-GT-333.

29. Ghenaiet, A et al, “Numerical Simulation of the Axial Fan Performance Degradation Due to the Ingestion of Sand”, *Proceedings of the ASME Turbo Expo 2002*, Jun 3-6, ASME Paper No. GT-2002-30644.

30. Gostelow, J.P., *Cascade Aerodynamics*, Pergamon Press, 1984.

31. Haq, Inamul and Saravanamuttoo, H.I.H., “Detection of Axial Compressor Fouling in High Ambient Temperature Conditions”, *Proceedings from the 1991 International Gas Turbine and Aeroengine Congress and Exposition*, Jun 1991, ASME Paper No. 91-GT-67.

32. Harris, L.P. and Spang, H.A.III, “Compressor Modeling and Active Control of Stall/Surge”, *Proceedings from the American Control Conference*, vol. 3, June 26-28, 1991, Boston, MA.

33. Haub, Barry L. and Hauhe, William E., “Field Evaluation of the On-Line Compressor Cleaning in Heavy Duty Industrial Gas Turbines”, *Proceedings from the 1990 International Gas Turbine and Aeroengine Congress and Exposition*.

34. Hayward, John, “Cleaning Method and Apparatus”, U.S. Patent #6,073,637.

35. Hill, Philip G. and Peterson, Carl R., *Mechanics and Thermodynamics of Propulsion*, Second Edition. Addison-Wesley Co, 1992.

36. Kolkman, H.J., “Performance of Gas Turbine Compressor Cleaners”, *Journal of Engineering for Gas Turbines and Power*, vol. 115, ASME Paper 92-GT-360.

37. Kurz, Rainer and Brun, Klaus, “Degradation in Gas Turbine Systems”, ASME Paper No. 2000-GT-345.

38. Leipold, R. et al, “The Influence of Technical Roughness Caused by Precision Forging on the Flow Around a Highly Loaded Compressor Cascade”, ASME Paper No. 99-GT-366.

39. Lindeburg, M.R., *Mechanical Engineering Reference Manual*, 11th Edition, Professional Publications, Inc, 2001.

40. Lofdahl, Jan-Olof, "35 Years of Operation With ROLLS-ROYCE Marine PROTEUS Gas Turbines in Swedish Navy Fast Surface Attack Ships", *Proceedings of the 1996 International Gas Turbine & Aeroengine Congress and Exhibition*, Jun 2-5, 1998, Stockholm, Sweden, ASME Paper # 98-GT-147.

41. Mal'tsev, Yu. N. and Shakhov, V.G., "Influence of Roughness of Deposits in Compressor Cascade on Flow Lag Angle", *Soviet Aeronautics*, vol. 32, no. 3, 1989.

42. Martin, Joe et al, "A Case For Compressor Coatings", *Turbomachinery International*, Dec 1998.

43. Mathioudakis, K. et al, "Fast Response Wall Pressure Measurement as a Means of Gas Turbine Blade Fault Identification", *Journal of Engineering for Gas Turbines and Power, Transactions of ASME*, vol. 113, no.2, Apr 1991.

44. Mathioudakis, K. et al, "Performance Analysis of Industrial Gas Turbines for Engine Condition Monitoring", *Proceedings from the Institution of Mechanical Engineers*, vol. 215, part A.

45. McDermott, Peter E., "Gas Turbine Compressor Fouling: The Case for On-Line Cleaning", *Turbomachinery International*, Jan/Feb 1991.

46. Meher-Homji, Cyrus B. (Boyce Eng. Int'l), "Gas Turbine Axial Compressor Fouling – A Unified Treatment of its Effects, Detection, and Control", *ASME - International Gas Turbine Institute Publication*, vol. 5, 1990.

47. Mezheritsky, A.D. and Sudarev, A.V., "Mechanism of Fouling and the Cleaning Technique in Application to Flow parts of the Power Generation Plant Compressors", *Proceedings from the 1990 International Gas Turbine and Aeroengine Congress and Exposition*, ASME Paper No. 90-GT-103.

48. Mezzedimi, Vasco et al, "CTV – A New Method for Mapping a Full Scale Prototype of an Axial Compressor", *Proceedings of the 1996 International Gas Turbine & Aeroengine Congress and Exhibition*, Jun 10-13, 1996, Burmingham, UK, ASME Paper # 96-GT-535.

49. Montazeri-Gh, et al, "Actuator Placement for Active Surge Control in a Multi-Stage Axial Compressor", *Proceedings of the 1996 International Gas Turbine & Aeroengine Congress and Exhibition*, Jun 10-13, Burmingham, UK, ASME Paper # 96-GT-241.

50. Najjar, Y.S.H., "Optimum Performance of a Simple Gas Turbine Engine Used as a Source of Compressed Air", *High Temperature Technology*, vol. 6, no. 1 Feb 1988.

51. Newman, W.H. et al, "Reduced Bleed Air Extraction for DC-10 Cabin Air Conditioning", *The 16th AIAA/SAE/ASME Jet Propulsion Conference*, Jun 30-Jul 2, 1980, Hartford, CT.

52. Ohnesorge, David H. et al, 1983, "Pressure Transducer", U.S. Patent #4,422,335.

53. *OPNAV INSTRUCTION 4790.16*, "Condition-Based Maintenance", 2000.

54. Orsagh, Rolf F. et al (Impact Tech & Carderock Div.), "Applications of Diagnostic & Prognostic Algorithms for Maintenance Optimization of Marine Gas Turbines", 2001.

55. Ozgur, Dincer et al, "Remote Monitoring and Diagnostics System for GE Heavy Duty Gas Turbines", *Proceedings from the 2000 International Gas Turbine and Aeroengine Congress and Exposition.*

56. Peltier, Robert V. and Swanekamp, Robert C., "LM2500 Recoverable and Non-Recoverable Power Loss", *Proceedings from the 1995 ASME Cogen-Turbo Power Conference,* ASME Paper No. 95-CTP-104.

57. Robbins, W.H. and Dugan, J.F., "Prediction of Off-Design Performance of Multi-Stage Compressors", *NASA SP-36*, 1965.

58. Roemer, Michael J. and Ghiocel, D.M., "A Probabilistic Approach to the Diagnosis of Gas Turbine Engine Faults", *53rd Machinery Prevention (MFPT) Conference Publication,* Apr 1999.

59. Roemer, Michael J. and Atkinson, Ben, "Real-Time Health Monitoring and Diagnostics for Gas Turbine Engines", *Proceedings from the 1997 International Gas Turbine and Aeroengine Congress and Exposition,* ASME Paper No. 97-GT-30.

60. Russom, D. and Jernoske, R, "U.S. Navy Rolls-Royce Allison 501-K34 Operating Experience", *ASME Turbo Expo Publication*, 2000.

61. Saravanamuttoo, H.I.H.; Matthee, F.A.H., "Development of a Low Cost Performance Monitoring System For Use On Board Naval Vessels", *Proceedings from the 1985 International Gas Turbine Conference and Exhibit*, London, England, ASME Paper # 82-GT-297.

62. Saravanamuttoo, H.I.H.; MacGillivray, P.J; Maclssac, B.D., "Development of Diagnostic Model for Marine Gas Turbines", *Proceedings from the 29th International Gas Turbine Conference and Exhibit*, Amsterdam, Netherlands, 1984.

63. Saravanamuttoo, H.I.H. and Baig, Mirza F., "Off-Design Performance Prediction of Single-Spool Turbojets using Gasdynamics", *Journal of Propulsion and Power*, vol. 13, no. 6, Nov-Dec 1997.

64. Saravanamuttoo, H.I.H.; Muir, D.E.; Marshall, D.J., "Health Monitoring of Variable Geometry Gas Turbines for the Canadian Navy", *Proceedings from the 1988 International Gas Turbine and Aeroengine Congress*, Amsterdam, Netherlands, ASME Paper # 88-GT-77.

65. Saravanamuttoo, H.I.H.; Aker, G.F., "Predicting Gas Turbine Performance Degradation Due to Compressor Fouling Using Computer Simulation Techniques", *Journal of Engineering for Gas Turbines and Power*, vol. 111, no. 2, 1989.

66. Saravanamuttoo, H.I.H. and Lakshminarasimha, A.N., "Prediction of Fouled Compressor Performance Using Stage Stacking Techniques", *Proceedings from the 4th Joint AIAA/ASME Fluid Mechanics, Plasma Dynamics and Lasers Conference*, vol. 37, 1986.

67. Saravanamuttoo, H.I.H. and Lakshminarasimha, A.N., "Preliminary Assessment of Compressor Fouling", *Turbomachinery International*, vol. 26, no. 7 Sep 1985.

68. Saravanamuttoo, H.I.H. and Seddigh, F., "Proposed Method for Assessing the Susceptibility of Axial Compressors to Fouling", *Proceedings from the 1990 International Gas Turbine and Aeroengine Congress and Exposition*, Jun 11-14, 1990, Brussels, Belgium, ASME Paper #GT-348.

69. Saravanamuttoo, H.I.H.; MacIsaac, B.D., "Thermodynamic Models for Pipeline Gas Turbine Diagnostics", *Journal of Engineering for Power, Transactions of ASME*, vol. 105, no. 4, 1983.

70. Schaffler, R., "Experimental and Analytical Investigation of the Effects of Reynolds Number and Blade Surface Roughness on Multistage Axial Flow Compressors", *Journal of Engineering for Power*, vol. 102, 1980.

71. Schlichting, H., *Boundary Layer Theory*, McGraw-Hill, Inc, 1987.

72. Scholz, N. and Klein, A., *Aerodynamics of Cascades*, AGARD Publication 1965/1977.

73. Scott, J.H., “Axial Compressor Monitoring By Measuring Intake Air Depression”, *Third Symposium on Gas Turbine Operations and Maintenance, National Research Council of Canada Symposium,* Sep 1979.

74. Sell, Robert C. et al, “Pressure Measuring System”, U.S. Patent #4,322,977.

75. Solomon, A., “Generic 1D Dynamic Modeling of a Gas Generator Engine”, *Proceedings of the 1997 International Gas Turbine & Aeroengine Congress and Exposition*, Jun 2-5, 1997, Orlando, FL, ASME Paper # 97-GT-28.

76. Song, T.W. et al, “Performance Prediction of Axial Flow Compressors Using Stage Characteristics and Simultaneous Calculation of Interstage Parameters”, *Proceedings of the Institution of Mechanical Engineers, Part A.: Journal of Power and Energy*, vol. 215, no. 1, 2001.

77. Stalder, Jean-Pierre and van Oosten, Peter, “Compressor Washing Maintains Plant Performance and Reduces Cost of Energy Production”, *Proceedings from the 1994 International Gas Turbine and Aeroengine Congress and Exposition*, June 1994, ASME Paper No. 94-GT-436.

78. Stalder, Jean-Pierre, “Gas Turbine Compressor Washing State of the Art – Field Experiences”, *Proceedings from the 1998 International Gas Turbine & Aeroengine Congress and Exhibition*, June 1998, ASME Paper No. 98-GT-420.

79. Sten’kin, E.D., “Operation of Compressor With Intermediate Bleed Air”, *Soviet Aeronautics* (English translation of *Izvestiya VUZ, Aviatsionnaya Tekhnika*), vol. 32, no.3, 1989.

80. Stone, A., “Effects of Stage Characteristics and Matching on Axial Flow Compressor Performance ”, *Transactions of ASME*, vol. 80, 1958.

81. Suder, K. et al, “The Effect of Adding Roughness and Thickness to a Transonic Axial Compressor Rotor”, *Journal of Turbomachinery*, vol. 117, Oct 1995.

82. Tarabrin, A.P. et al, “An Analysis of Axial Compressor Fouling and a Blade Cleaning Method”, *Journal of Turbomachinery*, vol. 120, Apr 1998, ASME Paper No. 96-GT-363.

83. Tarabrin, A.P. et al, “Influence of Axial Compressor Fouling on Gas Turbine Unit Performance Based on Different Schemes and With Different Initial Parameters”, ASME Paper No. 98-GT-416.

84. Tsalavoutas, A. et al, “Combining Advanced Data Analysis Methods for the Constitution of an Integrated Gas Turbine Condition Monitoring and Diagnostic System”, *Proceedings from the 2000 International Gas Turbine & Aeroengine Congress and Exhibition.*

85. Tsalavoutas, A. et al, "Identifying Faults in the Variable Geometry System of a Gas Turbine Compressor", *Journal of Turbomachinery*, vol. 123, Jan 2001, ASME Paper No. 2000-GT-33.

86. Walter, Hilger A. et al, 1996, "Process for Detecting Fouling of an Axial Compressor", U.S. Patent #5,479,818.

87. Watt, R. et al, "A Study of the Effects of Thermal Barrier Coating Surface Roughness on the Boundary Layer Characteristics of Gas Turbine Aerofoils", ASME Paper No. 87-GT-223.

88. White, Frank M., *Fluid Mechanics*, Fourth Edition. McGraw-Hill Co., 1999.

89. Williams, M.C. et al, "Analyses of Compressor Bleed Air", *Proceedings 75th APCA Annual Meeting*, New Orleans, LA, vol. 1, 1982.

90. Yeung, Simon et al, "Bleed Valve Rate Requirements Evaluation in Rotating Stall Control on Axial Compressors", *Journal of Propulsion and Power*, vol. 16, no. 5, Sep 2000.

91. Zaba, T., "Losses in Gas Turbines Due to Deposits on the Blading", *Brown Boveri Review*, vol. 67, no. 12 Dec 1980.

INITIAL DISTRIBUTION LIST

1. Defense Technical Information Center
   Ft. Belvoir, VA

2. Dudley Knox Library
   Naval Postgraduate School
   Monterey, CA

3. Department Chairman, Code ME
   Department of Mechanical Engineering
   Naval Postgraduate School
   Monterey, CA

4. Professor Knox. T. Millsaps, Jr., Code ME/Mi
   Department of Mechanical Engineering
   Naval Postgraduate School
   Monterey, CA

5. Program Officer
   Naval/Mechanical Engineering
   Naval Postgraduate School
   Monterey, CA

6. Mr. Jeffrey S. Patterson
   GT Emerging Technologies Section - Code 9334
   NSWC-Carderock, Philadelphia Detachment
   Philadelphia, PA

7. Mr. Daniel E. Caguiat
   GT Emerging Technologies Section - Code 9334
   NSWC-Carderock, Philadelphia Detachment
   Philadelphia, PA

8. Mr. John Scharschan
   GT Emerging Technologies Section - Code 9334
   NSWC-Carderock, Philadelphia Detachment
   Philadelphia, PA

9. Mr. Thomas Roche
   Manager, Gas Turbine Division
   NSWC-Carderock, Philadelphia Detachmen
   Philadelphia, PA

10. Mr. Ben Wainscott
Fleet Technical Support Center - Pacific
San Diego, CA

11. Mr. John Hartranft, Code 05Z-03
Naval Sea Systems Command
Washington Navy Yard, D.C.

12. Mr. Tim Hinrichs
Sr. Manager, Engineering
Rolls-Wood Group
San Leandro, CA

13. Mr. Mike Roemer
Impact Technologies, LLC.
Rochester, NY

14. Mr. Dennis M. Russom
Rolls Royce/Allison 501-K Gas Turbine
Life Cycle Engineer
NSWC-Carderock, Philadelphia Detachment
Philadelphia, PA

15. Mr. John J. Mcgroarty
Gas Turbine Condition Based Maintenance
Program Manager
NSWC-Carderock, Philadelphia Detachment
Philadelphia, PA